for ubiquitination assay instruction; and S. Sakiyama for reading the manuscript.

REFERENCES

1. Rosen, D. R., Siddique, T., Patterson, D., Figlewicz, D. A., Sapp, P., Hentati, A., Donaldson, D., Goto, J., O'Regan, J. P., Deng, H. X., Rahmani, Z., Krizus, A., McKenna-Yasek, D., Cayabyab, A., Gaston, S. M., Berger, R., Tanzi, R. E., Halperin, J. J., Herzfeldt, B., van den Bergh, R., Hung, W.-Y., Bird, T., Deng, G., Mulder, D. W., Smyth, C., Laing, N. G., Soriano, E., Pericak-Vance, M. A., Haines, J., Rouleau, G. A., Gusella, J. S., Horvitz, H. R., and Brown, R. H., Jr. (1993) *Nature* **364**, 59–62
2. Deng, H. X., Hentati, A., Tainer, J. A., Iqbal, Z., Cayabyab, A., Hung, W.-Y., Getzoff, E. D., Hu, P., Herzfeldt, B., Roos, R. P., Warner, C., Deng, G., Soriano, E., Smyth, C., Parge, H. E., Ahmed, A., Roses, A. D., Hallewell, R., Rericak-Vance, M. A., and Siddique, T. (1993) *Science* **261**, 1047–1051
3. Cleveland, D. W., and Liu, J. (2001) *Nat. Med.* **6**, 1320–1321
4. Brown, R. H., Jr., and Robberecht, W. (2001) *Semin. Neurol.* **21**, 131–139
5. Cluskey, S., and Ramsden, D. B. (2001) *Mol. Pathol.* **54**, 386–392
6. Orrell, R. W., and Figlewicz, D. A. (2001) *Neurology* **57**, 9–17
7. Keller, J. N., Huang, F. F., and Markesbery, W. R. (2000) *Neuroscience* **98**, 149–156
8. Hoffman, E. K., Wilcox, H. M., Scott, R. W., and Siman, R. (1996) *J. Neurol. Sci.* **139**, 15–20
9. Kunst, C. B., Mezey, E., Brownstein, M. J., and Patterson, D. (1997) *Nat. Genet.* **15**, 91–94
10. Hartmann, E., Gorlich, D., Kostka, S., Otto, A., Kraft, R., Knespel, S., Burger, E., Rapoport, T. A., and Prehn, S. (1993) *Eur. J. Biochem.* **214**, 375–381
11. Kato, S., Shimoda, M., Watanabe, Y., Nakashima, K., Takahashi, K., and Ohama, E. (1996) *J. Neuropathol. Exp. Neurol.* **55**, 1089–1101
12. Kato, S., Hayashi, H., Nakashima, K., Nanba, E., Kato, M., Hirano, A., Nakano, I., Asayama, K., and Ohama, E. (1997) *Am. J. Pathol.* **151**, 611–620
13. Nagai, M., Aoki, M., Miyoshi, I., Kato, M., Pasinelli, P., Kasai, N., Brown, R. H., Jr., and Itoyama, Y. (2001) *J. Neurosci.* **21**, 9246–9254
14. Nakagawara, A. (1998) *Med. Pediatr. Oncol.* **31**, 113–115
15. Harvey, K. F., and Kumar, S. (1999) *Trends Cell Biol.* **9**, 166–169
16. Kumar, S., Tomooka, Y., and Noda, M. (1992) *Biochem. Biophys. Res. Commun.* **30**, 1155–1161
17. Kato, S., Takikawa, M., Nakashima, K., Hirano, A., Cleveland, D. W., Kusaka, H., Shibata, N., Kato, M., Nakano, I., and Ohama, E. (2000) *Amyotroph. Lateral Scler. Other Motor Neuron Disord.* **1**, 163–184
18. Orrell, R. W. (2000) *Neuromuscul. Disord.* **10**, 63–68
19. Cudkowicz, M. E., McKenna-Yasek, D., Sapp, P. E., Chin, W., Geller, B., Hayden, D. L., Schoenfeld, D. A., Hosler, B. A., Horvitz, H. R., and Brown, R. H., Jr. (1997) *Ann. Neurol.* **41**, 210–221
20. Ratovitski, T., Corson, L. B., Strain, J., Wong, P., Cleveland, D. W., Culotta, V. C., and Borchelt, D. R. (1999) *Hum. Mol. Genet.* **8**, 1451–1460
21. Aoki, M., Ogasawara, M., Matsubara, Y., Narisawa, K., Nakamura, S., Itoyama, Y., and Abe, K. (1993) *Nat. Genet.* **5**, 323–324
22. Kato, M., Aoki, M., Ohta, M., Nagai, M., Ishizaki, F., Nakamura, S., and Itoyama, Y. (2001) *Neurosci. Lett.* **312**, 165–168
23. Andersen, P. M., Forsgren, L., Binzer, M., Nilsson, P., Ala-Hurula, V., Keranen, M. L., Bergmark, L., Saarinen, A., Haltia, T., Tarvainen, I., Kinnunen, E., Udd, B., and Marklund, S. L. (1996) *Brain* **119**, 1153–1172
24. Shibata, N., Hirano, A., Kobayashi, M., Siddique, T., Deng, H. X., Hung, W.-Y., Kato, T., and Asayama, K. (1996) *J. Neuropathol. Exp. Neurol.* **55**, 481–490
25. Sussman, D. J., Klingensmith, J., Salinas, P., Adams, P. S., Nusse, R., and Perrimon, N. (1994) *Dev. Biol.* **166**, 73–86
26. Wodarz, A., and Nusse, R. (1998) *Annu. Rev. Cell Dev. Biol.* **14**, 59–88
27. Boutros, M., Paricio, N., Strutt, D. I., and Mlodzik, M. (1998) *Cell* **94**, 109–118
28. Julien, J. P. (2001) *Cell* **104**, 581–591
29. Fons, R. D., Bogert, B. A., and Hegde, R. S. (2003) *J. Cell Biol.* **160**, 529–539
30. Fujita, Y., Okamoto, K., Sakurai, A., Gonatas, N. K., and Hirano, A. (2000) *J. Neurol. Sci.* **174**, 137–140
31. Mourelatos, Z., Gonatas, N. K., Stieber, A., Gurney, M. E., and Dal Canto, M. C. (1996) *Proc. Natl. Acad. Sci. U. S. A.* **93**, 5472–5477
32. Wharton, K. A., Jr. (2003) *Dev. Biol.* **253**, 1–17
33. Tsang, M., Lijam, N., Yang, Y., Beier, D. R., Wynshaw-Boris, A., and Sussman, D. J. (1996) *Dev. Dyn.* **207**, 253–262
34. Krylova, O., Messenger, M. J., and Salinas, P. C. (2000) *J. Cell Biol.* **151**, 83–94
35. Julien, J. P., and Beaulieu, J. M. (2000) *J. Neurol. Sci.* **180**, 7–14
36. Luo, Z. G., Wang, Q., Zhou, J. Z., Wang, J., Luo, Z., Liu, M., He, X., Wynshaw-Boris, A., Xiong, W. C., Lu, B., and Mei, L. (2002) *Neuron* **35**, 489–505
37. De Ferrari, G. V., and Inestrosa, N. C. (2000) *Brain Res. Brain Res. Rev.* **33**, 1–12
38. Kaytor, M. D., and Orr, H. T. (2000) *Curr. Opin. Neurobiol.* **12**, 275–278
39. Versteeg, R., Caron, H., Cheng, N. C., van der Drift, P., Slater, R., Westerveld, A., Voute, P. A., Delattre, O., Laureys, G., van Roy, N., and Speleman, F. (1995) *Eur. J. Cancer* **31**, 538–541
40. Murata, S., Minami, Y., Minami, M., Chiba, T., and Tanaka, K. (2001) *EMBO Rep.* **2**, 1133–1138
41. Okado-Matsumoto, A., and Fridovich, I. (2002) *Proc. Natl. Acad. Sci. U. S. A.* **99**, 9010–9014
42. Niwa, J., Ishigaki, S., Hishikawa, N., Yamamoto, M., Doyu, M., Murata, S., Tanaka, K., Taniguchi, N., and Sobue, G. (2002) *J. Biol. Chem.* **277**, 36793–36798
43. Mori, K. (2000) *Cell* **101**, 451–454
44. Travers, K. J., Patil, C. K., Wodicka, L., Lockhart, D. J., Weissman, J. S., and Walter, P. (2000) *Cell* **101**, 249–258
45. Wickner, S., Maurizi, M. R., and Gottesman, S. (1999) *Science* **286**, 1888–1893
46. Borchelt, D. R., Lee, M. K., Slunt, H. S., Guarnieri, M., Xu, Z. S., Wong, P. C., Brown, R. H., Jr., Price, D. L., Sisodia, S. S., and Cleveland, D. W. (1994) *Proc. Natl. Acad. Sci. U. S. A.* **16**, 8292–8296

THE JOURNAL OF BIOLOGICAL CHEMISTRY
Vol. 279, No. 24, Issue of June 11, pp. 25549–25561, 2004
Printed in U.S.A.

Polo-like Kinase 1 (Plk1) Inhibits p53 Function by Physical Interaction and Phosphorylation*

Received for publication, December 26, 2003, and in revised form, March 11, 2004
Published, JBC Papers in Press, March 15, 2004, DOI 10.1074/jbc.M314182200

Kiyohiro Ando‡§¶, Toshinori Ozaki‡¶, Hideki Yamamoto‡, Kazushige Furuya‡, Mitsuchika Hosoda‡, Syunji Hayashi‡, Masahiro Fukuzawa§, and Akira Nakagawara‡‖

From the ‡Division of Biochemistry, Chiba Cancer Center Research Institute, Chiba 260-8717, Japan and the §First Department of Surgery, Nihon University School of Medicine, Tokyo 173-8610, Japan

Polo-like kinase 1 (Plk1) has an important role in the regulation of M phase of the cell cycle. In addition to its cell cycle-regulatory function, Plk1 has a potential role in tumorigenesis. Here we found for the first time that Plk1 physically binds to the tumor suppressor p53 in mammalian cultured cells, and inhibits its transactivation activity as well as its pro-apoptotic function. During the cisplatin-induced apoptosis in human neuroblastoma SH-SY5Y cells, the expression level of Plk1 was significantly decreased both at mRNA and protein levels, whereas cisplatin treatment caused a remarkable stabilization of p53. Systematic immunoprecipitation analyses using a series of deletion mutants of p53 revealed that a sequence-specific DNA-binding region of p53 is required and sufficient for the physical interaction with Plk1. The ectopically overexpressed Plk1 was co-localized with the endogenous p53 in mammalian cell nucleus, as shown by confocal laser microscopy. Expression of exogenous Plk1 and p53 in p53-deficient lung carcinoma H1299 cells greatly decreased the p53-mediated transcription from the p53-responsive *p21*^{WAF1}, *MDM2*, and *BAX* promoters, whereas the kinase-deficient mutant form of Plk1 failed to reduce the transcriptional activity of p53. Consistent with the luciferase reporter analysis, Plk1 had an ability to block the p53-dependent induction of the endogenous p21^{WAF1}. In addition, Plk1 inhibited the pro-apoptotic function of p53 in H1299 cells. Intriguingly, Plk1-mediated repression of p53 was attenuated with ATM. Thus, our present findings strongly suggest that p53 is a critical target of Plk1, and its function is abrogated through the physical interaction with Plk1.

The polo-like kinases (Plks)[1] are structurally and functionally related to the *Drosophila* polo serine/threonine (Ser/Thr) kinase (1), and are evolutionarily well conserved from yeast to mammals. A high degree of amino acid sequence similarity is detected within a catalytic domain and a unique noncatalytic domain (termed the polo-box) located at the NH_2- and COOH-terminal region, respectively (2). It has been shown that the polo-box is critical for the correct subcellular localization of Plks (3, 4), and the COOH-terminal region containing the polo-box serves to regulate its kinase activity (5). A growing body of evidence obtained in various experimental systems suggests that Plks play an important role in the regulation of a variety of M-phase-specific events including entry into and exit from mitosis (1, 6–8). In addition to their critical role during the G_2/M transition, Plks might be also required for G_1/S phase transition (9, 10).

In mammalian cells, there exist at least three Plk family members including Plk1, Plk2, and Plk3. Plk1 (also referred to as Plk) has been identified as a serine/threonine kinase that displays an extensive amino acid sequence homology to *Drosophila* polo (2, 9, 11–13), whereas Plk2 (alternatively named Snk) and Plk3 (alternatively termed as proliferation related kinase, Prk) have been originally shown to be transcriptionally induced in response to mitogens (14, 15). In mammalian cultured cells, the amounts of Plk1 mRNA and protein are regulated in a cell cycle-dependent manner, rising from a very low level in G_1 phase to a maximal level during G_2/M phase (11, 12). The kinase activity of Plk1 is regulated by its phosphorylation and peaks at M phase (16–18). Recently, it has been shown that the kinase activity of Plk1 is inhibited in response to DNA damage in mammalian cultured cells and this inhibition occurs in an ATM-dependent manner (19, 20). Plk1 phosphorylates various substrate proteins including cyclin B1 and Cdc25C. At the onset of mitosis, Plk1 phosphorylated cyclin B1 and promoted rapid nuclear translocation of an active Cdc2-cyclin B1 complex (21, 22). In addition, Toyoshima-Morimoto *et al.* (23) has found that, during G_2/M phase, Plk1 is capable of phosphorylating Cdc25C, which dephosphorylates and directly activates the Cdc2-cyclin B1 complex, and regulating the nuclear entry of Cdc25C. In contrast to Plk1, the expression level of Plk3 remains constant during the cell cycle progression and its kinase activity peaks during late S and G_2 phase (24, 25). Xie *et al.* (26) found that the kinase activity of Plk3 is rapidly increased in response to DNA damage in an ATM-dependent fashion.

In addition to the potential cell cycle-regulatory role, Plk1 has been implicated in the genesis and/or progression of tumors. *Plk1* was overexpressed in rapidly proliferating cells as well as various human primary tumors (27), suggesting that the expression level of *Plk1* is tightly linked to proliferation and could be used as a negative prognostic indicator for various

* This work was supported in part by a grant-in-aid from the Ministry of Health and Welfare for a New 10-Year Strategy for Cancer Control, a grant-in-aid for Scientific Research on Priority Areas, a grant-in-aid for Scientific Research (B) from the Ministry of Education, Science, Sports and Culture, Japan, and the Hisamitsu Pharmaceutical Company. The costs of publication of this article were defrayed in part by the payment of page charges. This article must therefore be hereby marked "*advertisement*" in accordance with 18 U.S.C. Section 1734 solely to indicate this fact.

¶ Both authors contributed equally to this work.
‖ To whom correspondence should be addressed: Division of Biochemistry, Chiba Cancer Center Research Institute, 666-2 Nitona, Chuoh-ku, Chiba 260-8717, Japan. Tel.: 81-43-264-5431; Fax: 81-43-265-4459; E-mail: akiranak@chiba-ccri.chuo.chiba.jp.

[1] The abbreviations used are: Plk, polo-like kinase; ATM, ataxia telangiectasia mutated; GFP, green fluorescence protein; GST, glutathione *S*-transferase; NLS, nuclear localization signal; NMS, normal mouse serum; PBS, phosphate-buffered saline; TBS, Tris-buffered saline; TK, thymidine kinase; RT, reverse transcriptase.

tumors (28–30). Consistent with these observations, constitutive overexpression of Plk1 in NIH3T3 cells resulted in the oncogenic focus formation and induction of tumor growth in nude mice (10). Down-regulation of the endogenous *Plk1* by using several antisense oligonucleotides targeted to *Plk1* induced growth inhibition in certain cancerous cells (31). Additionally, treatment of the cells with small interfering RNA targeted against *Plk1* caused the cell cycle arrest and apoptosis (32, 33). Of note, Liu and Erikson (33) reported that the tumor suppressor p53 might be involved in the Plk1 depletion-induced apoptosis. Recently, Plk1 has also been reported to have an ability to phosphorylate p53 *in vitro*, however, it is still unknown whether there exists a functional association between Plk1 and p53 (26). In sharp contrast to *Plk1*, the expression level of *Plk3* was significantly down-regulated in several human primary tumors including lung carcinomas and head and neck squamous cell carcinomas, as compared with their corresponding normal tissues (34, 35). Overexpression of Plk3 in mammalian cultured cells inhibited proliferation and induced apoptosis (36). Furthermore, it has been demonstrated that Plk3 physically interacts with p53 and phosphorylates the Ser^{20} of p53, which might result in the enhancement of its activity. These suggest that Plk1 and Plk3 play a differential role in regulating cell proliferation and oncogenesis, and that p53 participates in Plk3-dependent growth inhibition and/or apoptosis (25, 26, 36, 37).

In the present study, we examined the physical and functional interaction between Plk1 and p53. We found that Plk1 binds to the sequence-specific DNA-binding domain of p53, and inhibits the p53-dependent transcriptional activation as well as pro-apoptotic function. Intriguingly, overexpression of ATM abrogated the Plk1-mediated inhibitory effect on p53. These results suggest that the Plk1-mediated negative regulation of p53 might be a fundamental mechanism for the Plk1-induced oncogenesis.

EXPERIMENTAL PROCEDURES

Tumor Samples—Surgically resected tumor tissues including three lung adenocarcinomas, two gastric adenocarcinomas, one uterus carcinoma, two bladder carcinomas, and their corresponding normal tissues used in this study were obtained as frozen specimens from the Tissue Bank in Chiba Cancer Center Hospital (Chiba, Japan). Six hepatoblastomas and their matched normal tissues were provided by the Japanese Study Group for Pediatric Liver Tumor.

Cell Culture—African green monkey kidney COS7 cells were maintained in Dulbecco's modified Eagle's medium supplemented with 10% heat-inactivated fetal bovine serum (Invitrogen) and penicillin (100 IU/ml)/streptomycin (100 μg/ml). Human neuroblastoma SH-SY5Y cells and human lung carcinoma H1299 cells were grown in RPMI 1640 medium containing 10% heat-inactivated fetal bovine serum and antibiotic mixture. Cultures were maintained at 37 °C in a water-saturated atmosphere of 5% CO_2 in air.

Transfection—COS7 cells were transfected with the indicated expression plasmids using FuGENE 6 transfection reagent (Roche Applied Science) in a 6-cm diameter culture dish in accordance with the manufacturer's specifications. Transfection of H1299 cells was conducted by lipofection with LipofectAMINE transfection reagent (Invitrogen) in a 12-well plate according to the manufacturer's instructions.

RT-PCR—Total RNA was prepared from SH-SY5Y cells exposed to cisplatin by using the RNeasy Mini Kit (Qiagen Inc., Valencia, CA) according to the manufacturer's protocol, and subjected to synthesis of the first strand cDNA with random primers and a SuperScript II reverse transcriptase (Invitrogen) at 42 °C for 1 h. When the reaction was complete, the cDNA was amplified in a final volume of 15 μl of reaction mixture containing 100 μM of each deoxynucleoside triphosphate, 1× PCR buffer, 1 μM of each primer, and 0.2 units of rTaq DNA polymerase (Takara, Ohtsu, Japan). The primers for *p53* amplification were 5′-ATTTGATGCTGTCCCCGGACGATATTGAAC-3′ and 5′-ACCCTTTTTGGACTTCAGGTGGCTGGAGTG-3′. The primers for $p21^{WAF1}$ amplification were 5′-ATGAAATTCACCCCCTTTCC-3′ and 5′-CCCTAGGCTGTGCTCACTTC-3′. The primers for *Plk1* amplification were 5′-ATCACCTGCCTGACCATTCCACCAAGG-3′ and 5′-AATTGCGGAAATATTTAAGGAGGGTGATCT-3′. The primers for *Plk3* amplification were 5′-GCGCGAGAAGATCCTAAATG-3′ and 5′-GATCTGCCGCAGGTAGTAGC-3′. The primers for *GAPDH* amplification were 5′-ACCTGACCTGCCGTCTAGAA-3′ and 5′-TCCACCACCCTGTTGCTGTA-3′. The PCR-amplified products were separated by electrophoresis on a 1.5% agarose gel and visualized by ethidium bromide post-staining.

Generation of FLAG-tagged Expression Constructs—The FLAG-tagged human *Plk1* construct was generated by PCR amplification using the cDNA derived from primary hepatoblastoma as a template. The forward and reverse primers used in the PCR were 5′-CCGCTCGAGAGTGCTGCAGTGACTGCAGGGAAG-3′ and 5′-CTAGTCTAGATTAGGAGGCCTTGAGACGGTTGCT-3′. The underlined nucleotides represent the XhoI restriction sites in the forward primer and the XbaI restriction site in the reverse primer. The PCR product was subcloned into pGEM-T Easy (Promega Corp., Madison, WI), and its nucleotide sequence was verified by automated dideoxy terminator cycle sequencing. The PCR product was digested with XhoI and XbaI, and inserted between the XhoI to XbaI sites in the pcDNA3-FLAG expression plasmid in-frame to the downstream of the FLAG tag to give pcDNA3-FLAG-*Plk1*.

Construction of the Deletion Mutants of p53 and Plk1—The *p53* deletion mutants, *p53*-(1–359), *p53*-(1–292), and *p53*-(1–101) were generated by using the forward primer 5′-CCCAAGCTTGGGATGGAGGAGCCGCAGTCAGATCCTAGCGTC-3′ (1F) in combination with the reverse primers 5′-CCGGAATTCCGGTCATGGCTCCTTCCCAGCCTGGGCATCCTT-3′ (359R), 5′-CCGGAATTCCGGTCATTTCTTGCGGAGATTCTCTTCCTCTGT-3′ (292R) and 5′-CCGGAATTCCGGTCATTTCTGGGAAGGGACAGAAGATGACA-3′ (101R), respectively. *p53*-(102–393) was amplified by using the forward primer 5′-CCCAAGCTTGGGATGACCTACCAGGGCAGCTACGGTTTCCGTCT-3′ (102F) and the reverse primer 5′-CCGGAATTCCGGTCAGTCTGAGTCAGGCCCTTCTGTCTTGAACAT-3′ (393R). Each of the forward and reverse primers contained the HindIII and EcoRI restriction sites to facilitate the subsequent cloning step. Underlined nucleotides in the oligonucleotides listed above were HindIII or EcoRI sites. Amplified fragments were digested with HindIII and EcoRI, and subcloned directly into the identical restriction sites of pcDNA3 to give pcDNA3-*p53*-(1–359), pcDNA3-*p53*-(1–292), pcDNA3-*p53*-(1–101), and pcDNA3-*p53*-(102–393). All of the constructs were confirmed by sequence analysis. For the construction of the deletion mutants of Plk1, pcDNA3-FLAG-*Plk1* was digested with BamHI, BamHI and BstXI, or BamHI and NcoI. A restriction fragment encoding amino acid residues 1–401, 1–329, or 1–98 was purified from agarose gels, filled in the overhangs with Klenow, and then inserted in-frame into the enzymatically modified BamHI and XhoI sites of the pcDNA3-FLAG expression plasmid to give pcDNA3-FLAG-*Plk1*-(1–401), pcDNA3-FLAG-*Plk1*-(1–329), or pcDNA3-FLAG-*Plk1*-(1–98), respectively. DNA sequencing confirmed the authenticity of the expression plasmids prior to transfection.

Construction of the Kinase-deficient Mutant Form of Plk1—The K82M mutation was introduced into wild-type Plk1 by the PCR-based strategy using *PfuUltra*™ High Fidelity DNA polymerase (Stratagene, La Jolla, CA) according to the manufacturer's instructions. The following oligonucleotides were used: 5′-ATGATTGTGCCTAAGTCTCTGCTGCTCAAGCCGCA-3′ (underlined segment encodes Met at amino acid position 82) and 5′-GCCCGCGAACACCTCCTTGGTGTCCGCGTCCGAGA-3′. Nucleic acid sequencing was performed to verify the presence of the desired mutation and absence of random mutations. The amplified fragment that contains the K82M mutation was then digested with HindIII and NcoI, gel-purified, and ligated with the NcoI/XbaI restriction fragment containing the 3′-portion of the wild-type *Plk1* cDNA. The resulting entire cDNA encoding the full-length Plk1 carrying the amino acid substitution at position 82 was inserted in-frame into the HindIII and XbaI sites of the pcDNA3-FLAG expression plasmid to give pcDNA3-FLAG-*Plk1*(K82M).

Construction of the Expression Plasmid for Antisense Plk1—A full-length human *Plk1* cDNA was ligated into the pcDNA3 expression plasmid in a reverse orientation to give As-*Plk1*, and the product was evaluated by restriction digestion. To assess the effect of As-*Plk1* on the endogenous Plk1, whole cell lysates prepared from H1299 cells transfected with As-*Plk1* were analyzed for Plk1 by immunoblotting.

GST Pull-down Assay—Whole cell lysates prepared from COS7 cells expressing FLAG-Plk1 were incubated with 1 μg of GST or GST-p53 (Santa Cruz Biotechnologies, Santa Cruz, CA) immobilized on glutathione-Sepharose beads for 2 h at 4 °C. The beads were washed extensively with NETN buffer (50 mM Tris-Cl, pH 7.5, 150 mM NaCl, 0.1% Nonidet P-40, and 1 mM EDTA) containing 1 mM phenylmethylsulfonyl fluoride. The bound proteins were eluted with 2× SDS sample buffer by boiling

for 5 min, and separated by 10% SDS-polyacrylamide gel electrophoresis followed by immunoblotting.

Immunofluorescent Labeling and Confocal Microscopy—COS7 cells, cultured onto glass coverslips, were transiently transfected with the expression plasmid for FLAG-Plk1. Transfected cells were washed twice with 1× PBS and then fixed with 1× PBS containing 3.7% formaldehyde for 30 min at room temperature. After washing with 1× PBS, cells were permeabilized with 0.2% Triton X-100 for 5 min at room temperature and blocked for 1 h in 1× PBS containing 3% bovine serum albumin. Cells were then incubated with polyclonal anti-p53 antibody (Cell Signaling Technology, Inc., Beverly, MA) and monoclonal anti-FLAG antibody (M2, Sigma) for 1 h at room temperature. After incubation with primary antibodies, cells were washed twice with 1× PBS and incubated with fluorescein isothiocyanate- or rhodamine-conjugated secondary antibodies (Invitrogen) diluted 1:200 for 1 h at room temperature. Cell nuclei were stained with 4,6-diamidino-2-phenylindole at a final concentration of 1 μg/ml (Sigma). Cells were finally washed with 1× PBS, the coverslips were removed from the dishes, mounted onto slides, and observed under Fluoview laser scanning confocal microscope (Olympus, Tokyo, Japan).

Western Blot Analysis—Cells were transfected with the indicated combinations of the expression plasmids. Forty-eight hours after transfection, cells were extracted directly with the lysis buffer containing 25 mM Tris-HCl, pH 8.0, 137 mM NaCl, 2.7 mM KCl, 1% Triton X-100, 1 mM phenylmethylsulfonyl fluoride and protease inhibitor mixture (Sigma) and the whole cell lysates were sonicated for 10 s followed by centrifugation at 15,000 rpm for 10 min at 4 °C to remove insoluble materials. The protein concentrations were determined using the Bradford protein assay according to the instructions of the vendor (Bio-Rad). Equal amounts of the whole cell lysates (50 μg of protein) were boiled in an SDS sample buffer consisting of 62.5 mM Tris-HCl, pH 6.8, 2% SDS, 2% β-mercaptoethanol, and 0.01% bromphenol blue and subjected to 10% SDS-polyacrylamide gel electrophoresis under reducing conditions and then electrotransferred onto Immobilon-P membranes (Millipore, Bedford, MA) at room temperature for 1 h. The membranes were blocked with TBS-T (50 mM Tris-Cl, pH 7.6, 100 mM NaCl, and 0.1% Tween 20) containing 5% nonfat dry milk at room temperature for 1 h, and subsequently incubated for 1 h with monoclonal anti-Plk1 (PL2 and PL6, Zymed Laboratories, Inc., San Francisco, CA), monoclonal anti-p53 (DO-1, Oncogene Research Products, Cambridge, MA), monoclonal anti-FLAG antibody (M2, Sigma), monoclonal anti-Plk3 antibody (B37–2, BD Pharmingen), polyclonal antibody specific for p53 phosphorylated at Ser^{15} (Cell Signaling, Beverly, MA), polyclonal anti-$p21^{WAF1}$ antibody (H-164, Santa Cruz Biotechnologies), or polyclonal anti-actin antibody (20–33, Sigma) in TBS-T, followed by an incubation with horseradish peroxidase-conjugated goat anti-mouse or anti-rabbit secondary antibody (Jackson ImmunoResearch Laboratories, West Grove, PA) diluted at 1:2,000 for 1 h at room temperature. The membranes were washed extensively with TBS-T and protein bands were visualized by enhanced chemiluminescence (ECL) according to the manufacturer's instructions (Amersham Biosciences).

Subcellular Fractionation—Cells were fractionated into cytosolic and nuclear fractions as described previously (38). Briefly, cells were washed twice with ice-cold 1× PBS and lysed in lysis buffer containing 10 mM Tris-HCl, pH 7.5, 1 mM EDTA, 0.5% Nonidet P-40, and a protease inhibitor mixture (Sigma) for 30 min at 4 °C. Cell lysates were centrifuged at 15,000 × *g* for 10 min to collect the soluble fraction as cytosolic extracts. Insoluble materials were washed with the lysis buffer and further dissolved in 1× SDS sample buffer to collect the nuclear fraction. The nuclear and cytoplasmic fractions were subjected to immunoblot analysis using the anti-FLAG, monoclonal anti-lamin B (Ab-1, Oncogene Research Products), or monoclonal anti-Ras (RASK-3, Seikagaku Co., Tokyo, Japan) antibody.

Immunoprecipitation and Western Blot Analysis—For the immunoprecipitation of Plk1 and p53, COS7 cells were transiently transfected with 2 μg of the expression plasmid for FLAG-Plk1 using FuGENE 6 transfection reagent. Forty-eight hours post-transfection, cells were harvested and lysed by incubation with mixing in 400 μl of the EBC buffer (50 mM Tris-HCl, pH 7.5, 120 mM NaCl, 0.5% Nonidet P-40, and 1 mM phenylmethylsulfonyl fluoride) at 4 °C for 30 min. Whole cell lysates were then subjected to centrifugation at 15,000 × *g* for 20 min at 4 °C to remove insoluble materials. Equal amounts of whole cell lysates were precleared with 30 μl of a 50% slurry of protein A-Sepharose (Amersham Biosciences). After centrifugation, the supernatant was incubated with the normal mouse serum (NMS), monoclonal anti-FLAG, or monoclonal anti-p53 antibody at 4 °C for 2 h. The immunocomplexes were precipitated with the protein A-Sepharose beads at 4 °C for 30 min, which were then pelleted by centrifugation at 15,000 × *g* for 5 min. The precipitates were washed with the lysis buffer three times at 4 °C, resuspended in 30 μl of the SDS sample buffer, and treated at 100 °C for 5 min. Proteins were then resolved by 10% SDS-polyacrylamide gel electrophoresis, and transferred onto the Immobilon-P membranes. The protein complex was detected by Western blot analysis using the monoclonal anti-FLAG or monoclonal anti-p53 antibodies.

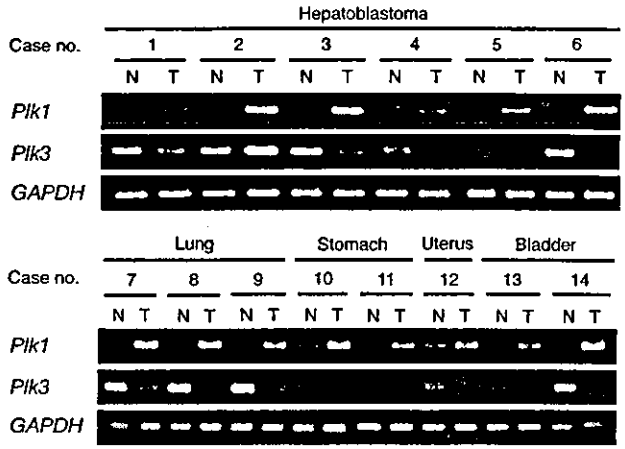

FIG. 1. **Expression of *Plk1* and *Plk3* mRNA in various human primary tumors and their corresponding normal tissues.** Total RNA (5 μg) prepared from the indicated tumor (*T*)-normal (*N*) paired samples was subjected to RT-PCR analysis for *Plk1* and *Plk3* mRNA expression using the specific primers as shown under "Experimental Procedures." The PCR-amplified products were analyzed by 1.5% agarose gel electrophoresis and visualized by ethidium bromide staining. Amplification of *GAPDH* was used as an internal control.

Luciferase Reporter Assays—p53-deficient H1299 cells were seeded in a 12-well tissue culture dish at a density of 5 × 10^4 cells/well. Cells were transfected with 100 ng of the p53-responsive luciferase reporter plasmid (*p21*, *MDM2*, or *BAX*), 10 ng of pRL-TK *Renilla* luciferase cDNA, and 25 ng of the expression plasmid for p53 together with or without increasing amounts of FLAG-Plk1 expression plasmid. The total amount of DNA was kept constant (510 ng) with pcDNA3 (Invitrogen) per transfection. Forty-eight hours post-transfection, transfected cells were washed twice with 1× PBS, and resuspended in passive lysis buffer (Promega Corp.). Both firefly and *Renilla* luciferase activities were assayed with the dual-luciferase reporter assay system (Promega Corp.) according to the manufacturer's instructions. The fluorescent light emission was determined by TD-20 luminometer (Turner Design, Sunnylvale, CA). The firefly luminescence signal was normalized based on the *Renilla* luminescence signal. The results were obtained from at least three sets of transfection and were presented as the mean ± S.D.

Cell Survival Assays—Cell viability was determined by a modified 3-(4,5-dimethylthiazol-2-yl)-2,5-diphenyltetrazolium bromide (MTT) assay. In brief, SH-SY5Y cells were seeded in 96-well microtiter plates (5 × 10^3 cell/well) with 100 μl of complete medium and allowed to attach. The next day, the medium were changed and cells were treated with cisplatin for 24 h. For the MTT assay, 10 μl of MTT solution was added to each well for 3 h at 37 °C. The absorbance readings for each well were carried out at 570 nm using the microplate reader (model 450, Bio-Rad).

Apoptotic Analysis—H1299 cells were transfected with a constant amount of the expression plasmid for green fluorescence protein (GFP) and p53 expression plasmid together with or without the expression plasmid encoding FLAG-Plk1. Forty-eight hours after transfection, transfected cells were identified by the presence of green fluorescence. To verify apoptosis, cell nucleus was stained with propidium iodide to reveal nuclear condensation and fragmentation. The number of GFP-positive cells with fragmented nuclei was scored, and presented as a percentage of the total number of fluorescent cells.

RESULTS

Expression of Plk1 and Plk3 in Paired Tumors and Adjacent Normal Tissues—It has been shown that the expression level of *Plk1* is increased in human tumors of various origins as compared with that of their corresponding normal tissues, suggesting that Plk1 contributes to the genesis and/or progression of tumors (13, 27–29). Recently, we have also identified *Plk1* as

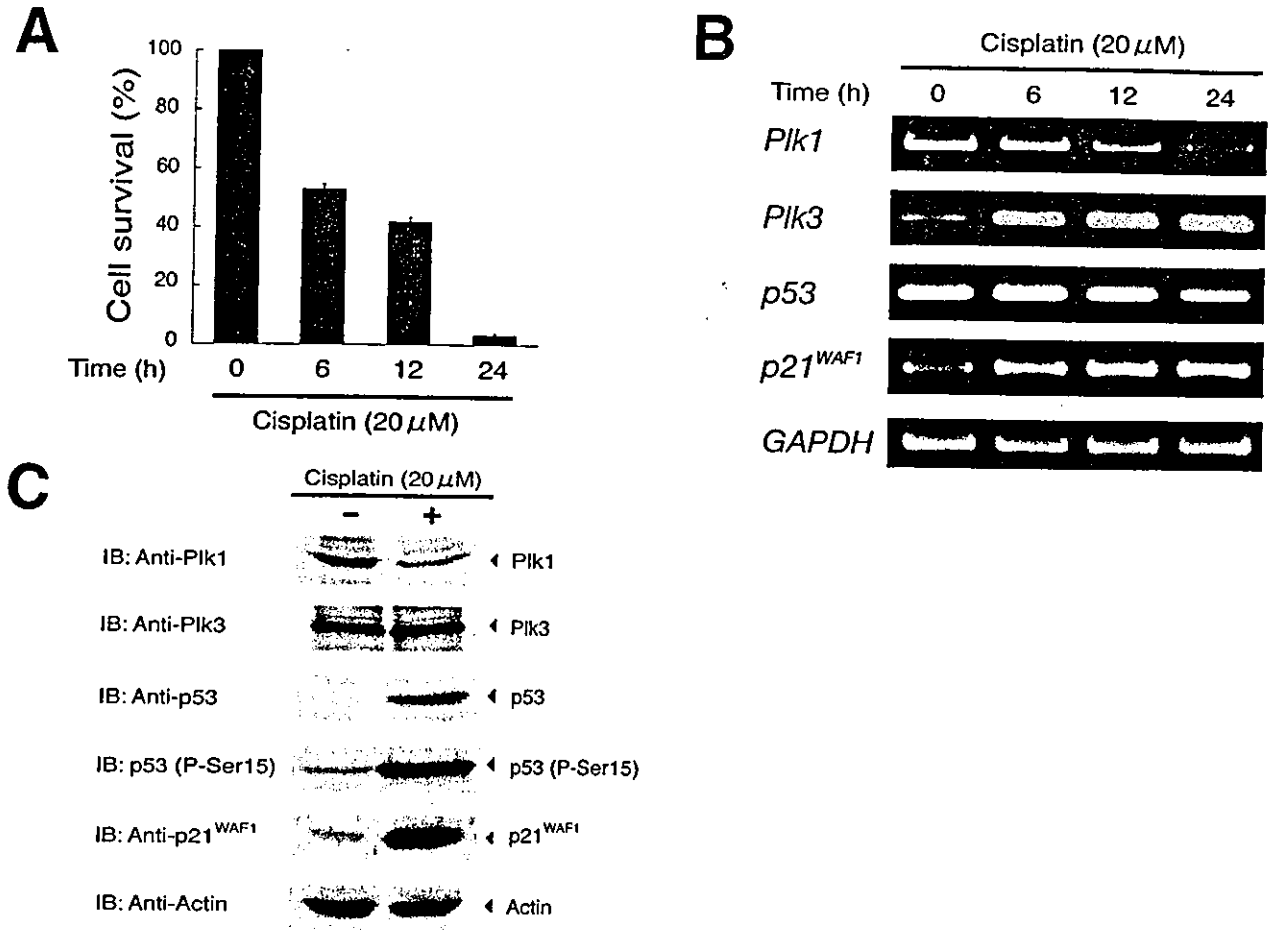

FIG. 2. **Down-regulation of *Plk1* during the cisplatin-induced apoptosis.** *A*, cell survival assays of SH-SY5Y cells treated with cisplatin. SH-SY5Y cells were exposed to cisplatin at a final concentration of 20 μM. At the indicated time periods after treatment with cisplatin, cell viability was determined by MTT assay. Data are presented as the mean ± S.D. of three independent experiments. *B*, RT-PCR analysis. Human neuroblastoma-derived SH-SY5Y cells were treated with or without cisplatin at a final concentration of 20 μM. At the indicated time periods after treatment with cisplatin, total RNA was prepared and subjected to RT-PCR analysis for the expression of *Plk1* (*1st panel*), *Plk3* (*2nd panel*), *p53* (*3rd panel*), and *p21*^{WAF1} (*4th panel*). Amplification of *GAPDH* serves as an internal control (*5th panel*). The PCR products were resolved in 1.5% agarose gels and visualized by ethidium bromide staining. *C*, Western blot analysis. Whole cell lysates were prepared from SH-SY5Y cells exposed to cisplatin for 24 h (at a final concentration of 20 μM) or left untreated and immunoblotted against anti-Plk1 (*1st panel*), anti-Plk3 (*2nd panel*), anti-p53 (*3rd panel*), antibody specific for p53 phosphorylated at Ser^{15} (*4th panel*), or with the anti-p21^{WAF1} antibody (*5th panel*). Immunoblotting for actin is shown as control for protein loading (*6th panel*).

one of the genes whose expression level is markedly elevated in human hepatoblastomas.[2] In contrast, *Plk3* expression is down-regulated in certain human tumors including lung carcinomas and head and neck squamous cell carcinomas (34, 35). To confirm the differential expression of both *Plk1* and *Plk3* in the same tissue samples, we examined their expression patterns among the indicated various paired cancer-normal tissues by RT-PCR. The levels of *GAPDH* mRNA were comparable between these paired samples. Consistent with the previous results, without exceptions, the expression levels of *Plk1* mRNA were significantly higher in cancerous tissues than those of their adjacent normal tissues (Fig. 1). On the other hand, *Plk3* was expressed at low levels in all the lung, uterus, and bladder carcinomas that we examined, as compared with their corresponding normal tissues, whereas a significant decrease in *Plk3* expression level in tumor tissues was undetectable in 2 of 6 hepatoblastomas and in 1 of 2 gastric carcinomas (Fig. 1). Thus, deregulated overexpression of *Plk1* is detected in all various types of tumors, whereas down-regulation of *Plk3* expression may be restricted to certain tumors.

Cisplatin Treatment Induces Down-regulation of Plk1 in Association with Up-regulation of p53 in SH-SY5Y Cells—To analyze whether Plk1 expression could be modulated during the cisplatin-induced apoptosis, whole cell lysates and total RNA were prepared from human neuroblastoma-derived SH-SY5Y cells after treatment with or without cisplatin, and were subjected to immunoblot analysis and RT-PCR, respectively. In accordance with our previous observations (39), cells underwent apoptosis in a time-dependent manner as measured by the cell survival assay (Fig. 2*A*), and a remarkable stabilization of p53 at the protein level was detected after treating the cells with cisplatin, accompanied with a significant up-regulation of p21^{WAF1} both at protein and mRNA levels (Fig. 2, *B* and *C*). In addition to the increase in the level of total p53, the phosphorylation of p53 at Ser^{15} was dramatically enhanced in cells exposed to cisplatin, whereas that of p53 at Ser^{20} was undetectable (data not shown). Intriguingly, cisplatin treatment markedly reduced the expression level of *Plk1* mRNA and protein (Fig. 2, *B* and *C*), suggesting that there exists an inverse relationship between the expression levels of p53 and Plk1 during DNA damage-induced apoptosis. Thus, Plk1 may play an important role in the p53 pathway. On the other hand, cisplatin treatment resulted in a significant up-regulation of *Plk3* mRNA expression in a time-dependent manner, however,

[2] Yamada, S., Ohira, M., Horie, H., Ando, K., Takayasu, H., Suzuki, Y., Sugano, S., Hirata, T., Goto, T., Matsunaga, T., Hiyama, E., Hayashi, Y., Ando, H., Suita, S., Kaneko, M., Sakaki, F., Hashizume, K., Ohnuma, N., and Nakagawara, A. (2004) *Oncogene*, in press.

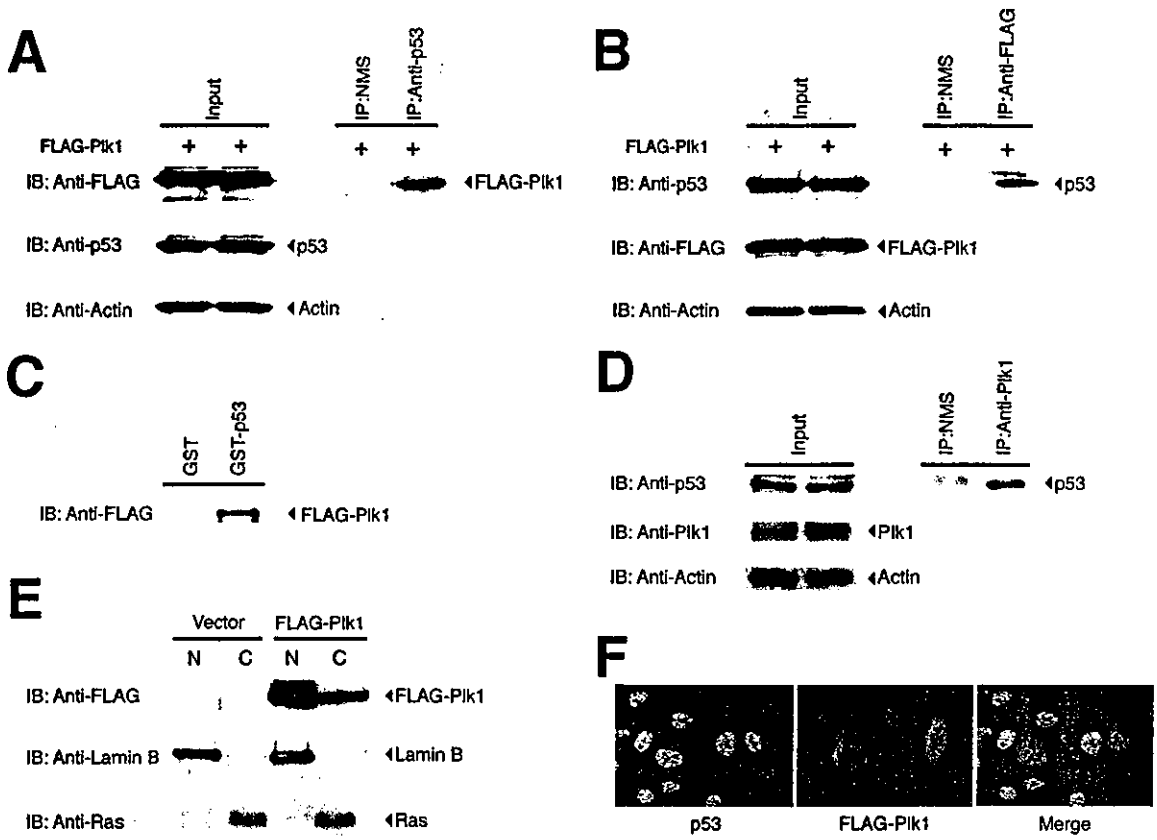

FIG. 3. **Co-immunoprecipitation and nuclear co-localization of Plk1 and p53.** *A*, complex formation between Plk1 and p53 in mammalian cultured cells. COS7 cells were transiently transfected with the expression plasmid for FLAG-tagged Plk1. Forty-eight hours after transfection, whole cell lysates were prepared and immunoprecipitated (*IP*) with NMS or with monoclonal anti-p53 antibodies. The immunocomplexes were resolved by 10% SDS-polyacrylamide gel electrophoresis and immunoblotted (*IB*) with monoclonal anti-FLAG antibody. Whole cell lysates were immunoblotted with monoclonal anti-p53, or with monoclonal anti-FLAG antibody to show the expression of endogenous p53, or FLAG-Plk1, respectively. The p53 blot was reprobed for actin to ensure equal loading. *B*, a similar immunoprecipitation assay was performed with NMS or monoclonal anti-FLAG antibody, followed by immunoblotting with monoclonal anti-p53 antibody. Whole cell lysates were monitored on immunoblot for the expression of endogenous p53 or FLAG-Plk1. The p53 blot was reprobed for actin to ensure equal loading. *C*, GST pull-down assay. Whole cell lysates prepared from COS7 cells expressing FLAG-Plk1 were incubated with GST or GST-p53 immobilized on glutathione-Sepharose beads. The bound proteins were separated by 10% SDS-polyacrylamide gel electrophoresis, and subjected to immunoblotting with the anti-FLAG antibody. *D*, association between endogenous p53 and Plk1. Cell lysates prepared from U2OS cells were immunoprecipitated with NMS or with monoclonal anti-Plk1 antibody, and the anti-Plk1 immunoprecipitates were immunoblotted with monoclonal anti-p53 antibody. *E*, subcellular localization of Plk1. COS7 cells were transiently transfected with the expression plasmid encoding FLAG-Plk1. Forty-eight hours after transfection, cells were fractionated into nuclear (*N*) and cytosolic (*C*) fractions as described under "Experimental Procedures." Equal amounts of each fraction were resolved by 10% SDS-polyacrylamide gel electrophoresis and immunoblotted with monoclonal anti-FLAG antibody (*top panel*). These extracts were also immunoblotted with monoclonal antibody specific for lamin B (*middle panel*) or Ras (RASK-3) (*bottom panel*) to show the validity of our fractionation technique. *F*, nuclear co-localization of Plk1 and p53. COS7 cells were transiently transfected with the FLAG-Plk1 expression plasmid. Following transfection, cells were fixed and incubated with polyclonal anti-p53 and monoclonal anti-FLAG antibodies that were revealed by fluorescein isothiocyanate-conjugated anti-rabbit IgG (*green*) and rhodamine-conjugated anti-mouse IgG (*red*), respectively. Merge analysis (*yellow*) showed the nuclear co-localization of Plk1 and p53.

the amount of Plk3 protein remained constant, regardless of cisplatin treatment.

Interaction of Plk1 with p53—Recently, it has been shown that Plk3 interacts with p53 and is directly involved in the stress-induced phosphorylation of p53 on the serine 20 residue (25, 26, 36, 37). Of note, Xie *et al.* (26) found that Plk1 is able to phosphorylate p53 *in vitro*, however, its functional significance *in vivo* remains unclear. These observations prompted us to investigate possible interactions between Plk1 and p53. For this purpose, COS7 cells, which express a large amount of endogenous p53 (40), were transiently transfected with the expression plasmid for FLAG-tagged Plk1. Whole cell lysates prepared from the transfected cells were immunoprecipitated with NMS or with a monoclonal anti-p53 antibody, and the immunoprecipitates were analyzed by immunoblotting with a monoclonal anti-FLAG antibody. As shown in Fig. 3*A*, FLAG-Plk1 was co-immunoprecipitated with the endogenous p53, but not present in the control immunoprecipitates obtained with the normal mouse serum. The expression of FLAG-Plk1 and the endogenous p53 was confirmed by immunoblot analysis with the antibody against the FLAG epitope and p53, respectively (Fig. 3*A*). Analysis of the anti-FLAG immunoprecipitates also revealed that p53 is co-immunoprecipitated with FLAG-Plk1 (Fig. 3*B*). To confirm their interaction *in vitro*, GST pull-down experiments were performed using GST fusion full-length human p53. As shown in Fig. 3*C*, mammalian expressed FLAG-Plk1 bound to GST-p53 but not to GST alone. Their interaction was further examined using endogenous materials. Whole cell lysates prepared from U2OS cells that carry wild-type p53 (41) were immunoprecipitated with a monoclonal anti-Plk1 antibody and the anti-Plk1 immunoprecipitates were analyzed for the presence of the endogenous p53. As shown in Fig. 3*D*, the endogenous p53 was co-immunoprecipitated with the endogenous Plk1. Similar results were also obtained in HeLa cells (data not shown). These results clearly demonstrate that Plk1 interacts with p53 in mammalian cultured cells and *in vitro*.

To evaluate the subcellular localization of Plk1, we per-

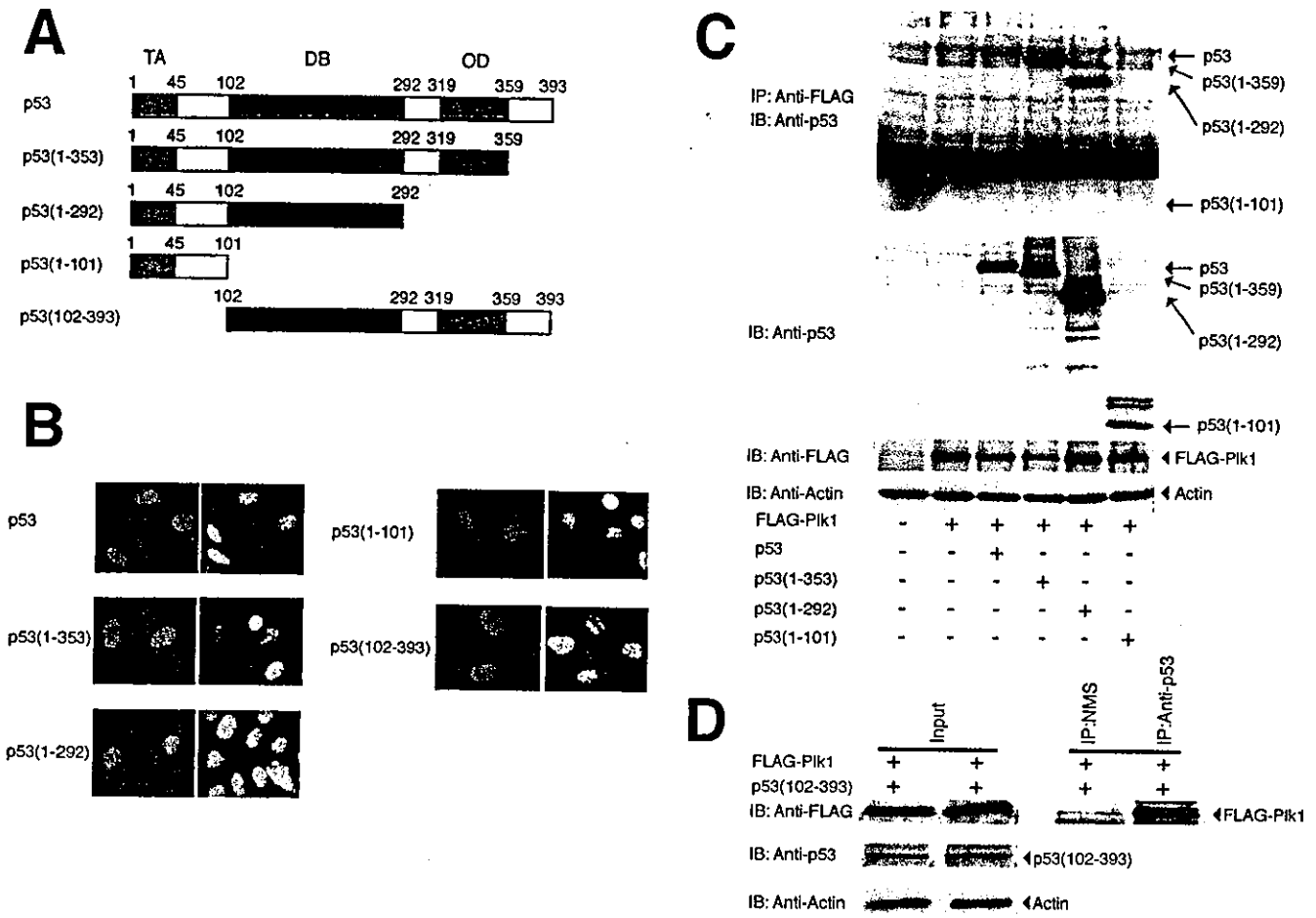

FIG. 4. **DNA-binding domain of p53 is required for interaction with Plk1.** *A*, schematic drawing of full-length p53 and various deletion mutants used in this study. *TA*, transactivation domain; *DB*, sequence-specific DNA-binding domain; *OD*, oligomerization domain. *Numbers* indicate amino acid position. *B*, subcellular localization of various deletion mutants of p53. *p53*-deficient H1299 cells were transiently transfected with the indicated expression plasmids. Forty-eight hours after transfection, cells were fixed and incubated with monoclonal anti-p53 antibody (DO-1 or PAb 421). Cell nuclei were stained with 4,6-diamidino-2-phenylindole (*blue*). Expression of p53 derivatives was visualized with rhodamine-conjugated secondary antibody (*red*). *C* and *D*, Plk1 interacts with the DNA-binding domain of p53. H1299 cells were transiently co-transfected with the indicated combinations of the expression plasmids. Forty-eight hours after transfection, whole cell lysates were prepared and subjected to immunoprecipitation with monoclonal anti-FLAG antibody followed by immunoblotting with monoclonal anti-p53 antibody (*upper panel*). The *lower panels* show the direct immunoblot analyses of whole cell lysates performed with monoclonal anti-p53, monoclonal anti-FLAG, or with polyclonal anti-actin antibody (*C*). Whole cell lysates from H1299 cells overexpressing FLAG-Plk1 and p53-(102–393) were immunoprecipitated with monoclonal anti-p53 antibody (PAb421) or with NMS followed by immunoblotting with monoclonal anti-FLAG antibody. Expression levels of p53-(102–393), FLAG-Plk1, and actin were examined by immunoblotting (*D*).

formed indirect immunofluorescent staining as well as biochemical cell fractionation of the transfected COS7 cells. COS7 cells transfected with the empty plasmid or with the expression plasmid for FLAG-Plk1 were fractionated into cytoplasmic and nuclear fractions for immunoblot analysis of FLAG-Plk1. Ras and lamin B served as markers for the purity of cytoplasmic and nuclear fractions, respectively (Fig. 3*E*, *lower panels*). Consistent with previous observations (10, 22, 42), FLAG-Plk1 was detected both in the cytoplasm and nucleus (Fig. 3*E*, *upper panel*). For immunofluorescent staining, COS7 cells expressing FLAG-Plk1 were fixed and stained with monoclonal anti-FLAG and polyclonal anti-p53 antibodies. As shown in Fig. 3*F*, FLAG-Plk1 localized to both the cytoplasm and nucleus. Merging analysis by confocal microscopy showed that FLAG-Plk1 co-localizes with endogenous p53 in cell nucleus.

The Sequence-specific DNA-binding Region of p53 Is Required for the Interaction with Plk1—To assess regions of p53 involved in the interaction with Plk1, we constructed a series of p53 deletion mutants including p53-(1–359) (lacking an extreme COOH-terminal region), p53-(1–292) (lacking the most COOH-terminal region including an oligomerization domain), p53-(1–101) (retaining only an NH_2-terminal transactivation domain), and p53-(102–393) (lacking an NH_2-terminal transactivation domain) (Fig. 4*A*). We first examined their subcellular localization by indirect immunofluorescent staining. To this end, p53-deficient human lung carcinoma H1299 cells (43) were transiently transfected with each expression plasmid. Forty-eight hours after transfection, cells were fixed and stained with the appropriate monoclonal anti-p53 antibody. As described previously (44, 45), there exist three potential nuclear localization signals (NLS I, II, and III) in the COOH-terminal region of p53, and NLS I alone has an ability to translocate the pyruvate kinase fusion protein to the nucleus. As shown in Fig. 4*B*, wild-type p53 and p53-(102–393), which retain the intact COOH-terminal region, accumulated in the nucleus. In addition, p53-(1–359), which lacks the NLS II and III but retains the NLS I, localized largely in the nucleus. On the other hand, p53-(1–292) and p53-(1–101), which lack three potential NLSs, were detected both in the nucleus and the cytoplasm. We then examined their abilities to interact with Plk1. H1299 cells were transiently co-transfected with the FLAG-Plk1 expression plasmid along with the expression plasmid for wild-type p53, p53-(1–359), p53-(1–292), or p53-(1–101), and the anti-FLAG immunoprecipitates were analyzed for the presence of wild-

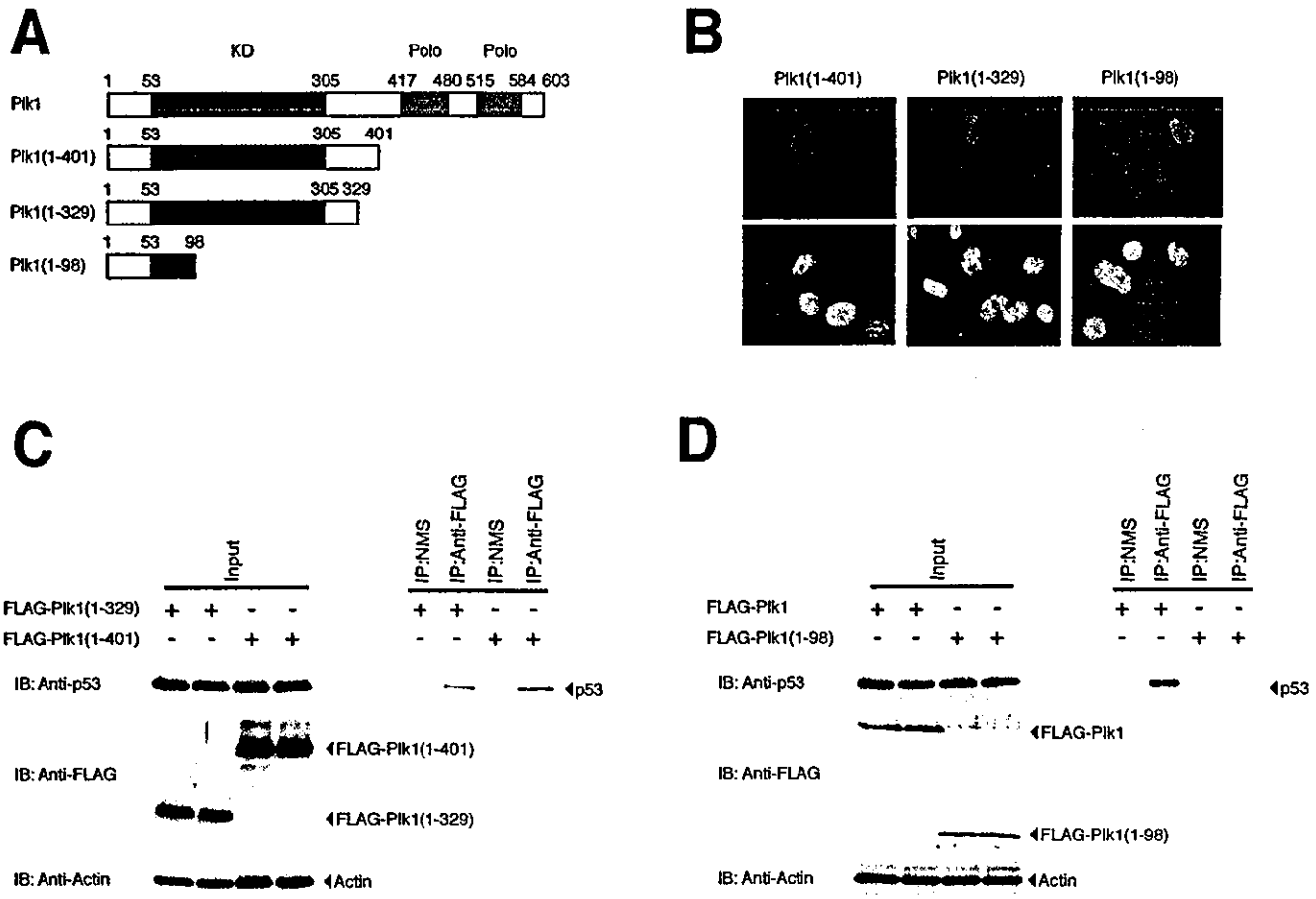

FIG. 5. **Mapping of the region of Plk1 required for interaction with p53.** *A*, schematic representation of Plk1 deletion mutants. *KD*, kinase domain; *Polo*, polo-box. *Numbers* indicate amino acid position. *B*, immunofluorescent studies of Plk1 deletion mutants. Transfected COS7 cells were fixed in 3.7% formaldehyde for 30 min, permeabilized with 0.2% Triton X-100 for 5 min, and blocked in PBS containing 3% bovine serum albumin for 1 h. Cells were then incubated with monoclonal anti-FLAG antibody followed by incubation with rhodamine-conjugated secondary antibody (*red*), and analyzed by confocal microscopy. Cell nuclei were stained with 4,6-diamidino-2-phenylindole (*blue*). *C* and *D*, interaction between various Plk1 deletion mutants and endogenous p53. Whole cell lysates from COS7 cells transfected with the indicated expression plasmids were immunoprecipitated with monoclonal anti-FLAG antibody, and immunoblotted with monoclonal anti-p53 antibody to observe the interaction between Plk1 deletion mutants and p53. Immunoprecipitation with NMS was used as a negative control. Equal amounts of protein derived from cell lysates were immunoblotted with monoclonal anti-p53, monoclonal anti-FLAG, or polyclonal anti-actin antibody.

type p53 and these truncated forms of p53. As shown in Fig. 4*C*, wild-type p53 as well as p53 deletion mutants including p53-(1–359) and p53-(1–292), were detected in the anti-FLAG immunoprecipitates, whereas p53-(1–101) has lost the ability to bind to Plk1, indicating that the extreme COOH-terminal region, the oligomerization domain, and the NH_2-terminal transactivation domain of p53 are not involved in the interaction with Plk1. Similar immunoprecipitation analyses revealed that p53-(102–393) co-precipitates with FLAG-Plk1 (Fig. 4*D*). Thus, the region between amino acid residues 102 and 292 of p53, which includes the sequence-specific DNA-binding domain, appears to be required and sufficient for the interaction with Plk1.

Mapping of the p53-binding Region of Plk1—To map the p53-interacting domain on Plk1, we have constructed the FLAG-tagged Plk1 deletion mutants including Plk1-(1–401), Plk1-(1–329), and Plk1-(1–98) (Fig. 5*A*), and examined their subcellular localization by indirect immunofluorescent staining. As shown in Fig. 5*B*, COS7 cells transfected with each of the expression plasmids for FLAG-tagged Plk1 deletion mutants exhibited intense staining of the nucleus. Inspection of the amino acid sequence of Plk1-(1–98) identified one cluster of basic amino acids (^{48}RSRRRYVRGR^{57}), suggesting that this basic cluster acts as a nuclear localization signal. We then tested the interaction between p53 and each of these Plk1 deletion mutants. COS7 cells were transfected with the expression plasmid encoding Plk1-(1–401), Plk1-(1–329), or Plk1-(1–98), and co-immunoprecipitation experiments were performed to determine the interaction. We found that Plk1-(1–401) and Plk1-(1–329) retained the ability to bind to p53, whereas Plk1-(1–98) did not (Fig. 5*C*). These results indicate that the amino acid sequence comprising residues 99 to 329 of Plk1 contains the p53-binding domain.

Plk1 Inhibits the p53-mediated Transcriptional Activation—To determine whether Plk1 could affect the transcriptional activity of p53, H1299 cells were transiently co-transfected with a constant amount of the expression plasmid encoding p53 together with the p53-responsive *p21^{WAF1}*, *MDM2*, or *BAX*-luciferase reporter constructs in the presence or absence of increasing amounts of the expression plasmid for FLAG-Plk1. Under our experimental conditions, ectopically expressed p53 successfully activated the transcription of each of those p53-responsive reporters as compared with the empty plasmid controls, but Plk1 alone had no effect on luciferase activity (Fig. 6). Expression of FLAG-Plk1 greatly reduced the ability of p53 to increase the *p21^{WAF1}*-, *MDM2*-, and *BAX*-luciferase activities in a dose-dependent manner (Fig. 6, *A–C*). In addition, Plk1-(1–98), which lacks an ability to interact with p53, did not affect the p53 transcriptional activity toward the *p21^{WAF1}*, *MDM2*, and *BAX* promoters (data not shown). To confirm the inhibitory role of Plk1 in the p53-mediated transactivation, we assayed H1299 cell transfectants for induction of the endoge-

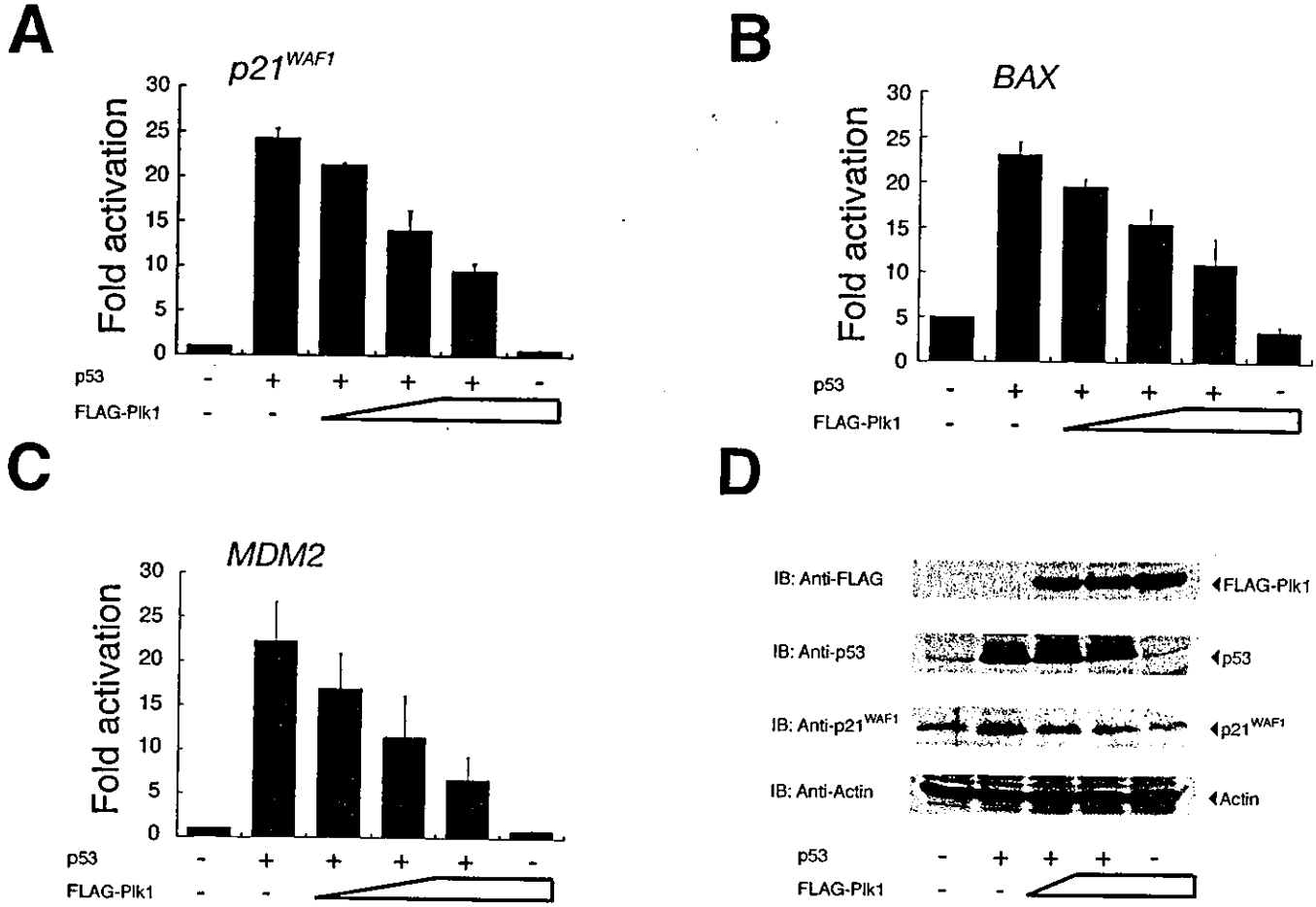

FIG. 6. **Plk1 abrogates the p53-mediated transcriptional activation.** *p53*-deficient H1299 cells (5×10^4 cells/well) were transiently co-transfected with 25 ng of the expression plasmid for p53 together with 100 ng of the luciferase reporter construct that carries the p53-responsive element derived from $p21^{WAF1}$ (*A*), *BAX* (*B*), or *MDM2* (*C*) promoter and 10 ng of the *Renilla* luciferase plasmid (pRL-TK) in the presence or absence of increasing amounts of pcDNA3-FLAG-Plk1 (50, 100, or 200 ng). The total amount of plasmid DNA per transfection was kept constant (510 ng) with pcDNA3. All transfections were performed in triplicate. Forty-eight hours after transfection, cells were lysed, and analyzed for their luciferase activities. Firefly luminescence signal was normalized based on the *Renilla* luminescence signal. Results are shown as -fold induction of the firefly luciferase activity compared with control cells transfected with pcDNA3 alone. *D*, immunoblot analysis. H1299 cells were transiently co-transfected with the indicated combinations of expression plasmids. Whole cell lysates were prepared 48 h post-transfection, and analyzed for the expression of FLAG-Plk1 (*1st panel*), p53 (*2nd panel*), or $p21^{WAF1}$ (*3rd panel*) by immunoblot analysis with monoclonal anti-FLAG, monoclonal anti-p53, or polyclonal anti-$p21^{WAF1}$ antibody, respectively. Total protein levels were controlled with polyclonal anti-actin antibody (*4th panel*).

nous $p21^{WAF1}$. To this end, H1299 cells were transiently co-transfected with a constant amount of the expression plasmid for p53 together with or without increasing amounts of the FLAG-Plk1 expression plasmid. Forty-eight hours after transfection, whole cell lysates were prepared and subjected to immunoblot analysis. Equal protein loading was confirmed by immunoblotting with the antibody against actin. As described (46), overexpression of p53 in H1299 cells resulted in the induction of the endogenous $p21^{WAF1}$ compared with basal levels seen with empty plasmid (Fig. 6*D*, *first* and *second lanes*). Co-expression of p53 with FLAG-Plk1 caused a significant decrease in the endogenous $p21^{WAF1}$ level in a dose-dependent manner (Fig. 6*D*, *third* and *fourth lanes*). These findings strongly suggest that Plk1 has an ability to inhibit p53-mediated transcriptional activation through physical interaction with p53.

To assess the possible effect of the endogenous Plk1 on the transcriptional activity of p53, we have employed an antisense strategy. As shown in Fig. 7*A*, expression of antisense *Plk1* in H1299 cells resulted in a reduction of the endogenous Plk1 as detected by immunoblot analysis. We then performed luciferase reporter analysis utilizing H1299 cells. As expected, co-expression of p53 with the antisense *Plk1* led to a slight but significant increase in the p53-mediated transcriptional activation as compared with cells expressing p53 alone (Fig. 7, *B–D*).

Plk1 Inhibits the p53-mediated Apoptosis—To extend the functional significance of the physical interaction between Plk1 and p53, we next determined whether Plk1 could affect p53-mediated apoptosis. H1299 cells were transiently co-transfected with the expression plasmid encoding p53 together with or without the expression plasmid for FLAG-Plk1. Forty-eight hours after transfection, cell viability was monitored by a cell survival assay. As shown in Fig. 8*A*, overexpression of p53 resulted in a reduction of the number of viable cells as compared with that found in the control transfection, and Plk1 alone had little effect on cell viability. The reduced number of viable cells caused by exogenous p53 was recovered by co-expression of FLAG-Plk1. Considering that p53 induced apoptosis in transfected H1299 cells (47), Plk1 might abrogate the pro-apoptotic function of p53. To confirm this possibility, H1299 cells were transiently co-transfected with a constant amount of the GFP expression plasmid together with the indicated combinations of the expression plasmids. Forty-eight hours after transfection, transfected cells were scored by fluorescence microscopy for the appearance of green fluorescence,

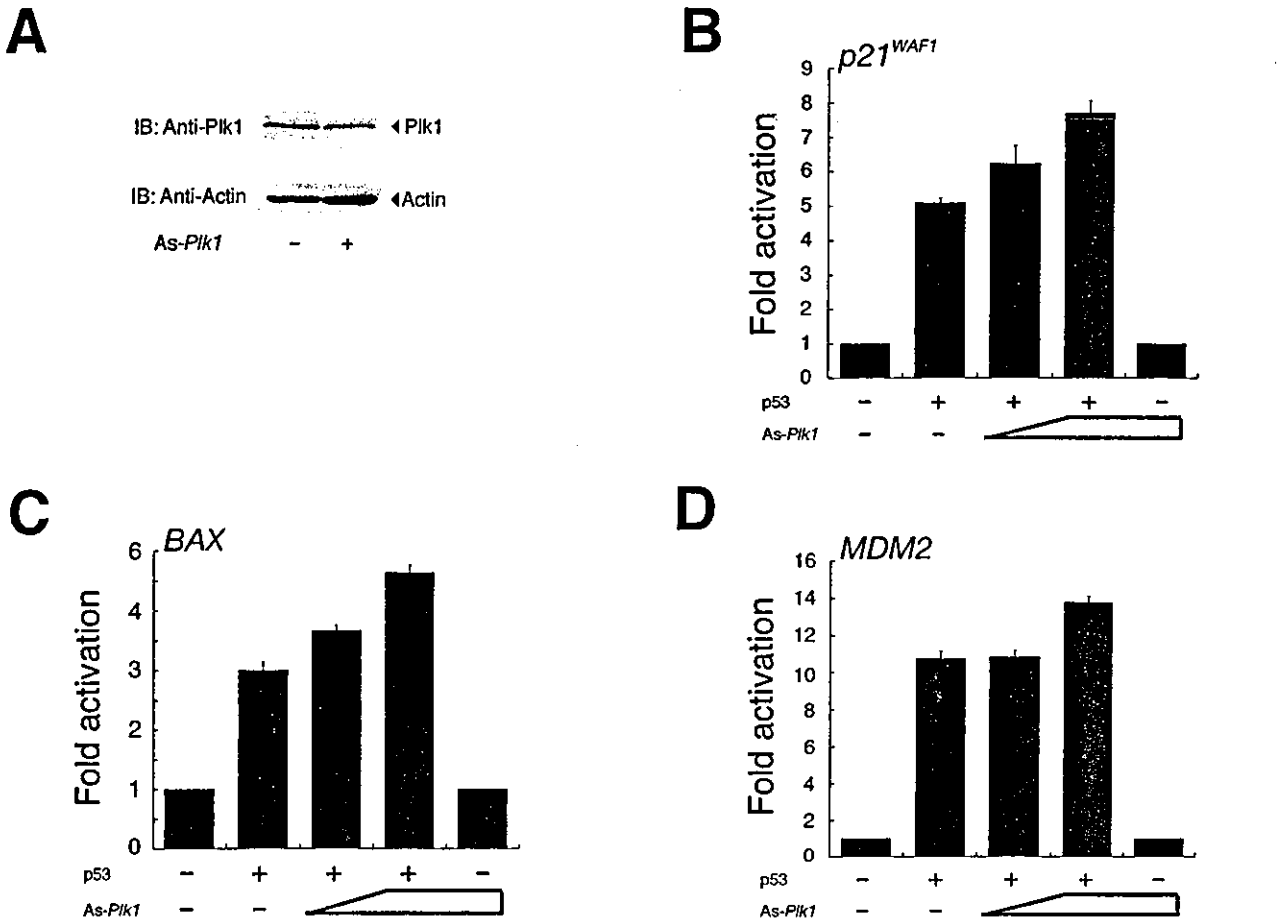

FIG. 7. **Antisense *Plk1* increases the transcriptional activity of p53.** *A*, antisense *Plk1* expression in H1299 cells results in a reduction of endogenous Plk1. H1299 cells were transfected with 2 μg of antisense *Plk1* expression plasmid (*As-Plk1*). Whole cell lysates prepared from transfected cells were subjected to immunoblotting with the anti-Plk1 antibody (*top panel*). Western blotting for actin is shown as a control for protein loading (*bottom panel*). *B–D*, luciferase reporter analysis. H1299 cells were transiently co-transfected with 12.5 ng of the p53 expression plasmid along with 100 ng of the indicated luciferase reporter construct in the presence or absence of increasing amounts of As-*Plk1* (200 and 400 ng). Determination and calculation of the luciferase activities are described in the legend to Fig. 6.

and the number of GFP-positive cells with condensed and fragmented nuclei were counted. Under our experimental conditions, enforced expression of p53 led to an increase in the number of apoptotic cells as compared with the control transfection (Fig. 8*B*). In agreement with the above cell survival assay, co-expression of p53 with FLAG-Plk1 decreased the number of apoptotic cells as compared with that resulting from expression of p53 alone. Taken together, these results indicate that Plk1 is an efficient inhibitor of p53.

Kinase-deficient Plk1 Fails to Inhibit p53—Next, we tested whether the Plk1 kinase activity could be required for Plk1-dependent inhibition of the p53 transcriptional activity. As described previously (22), the mutant form of Plk1 (Plk1-K82M), in which Lys^{82} within the ATP-binding motif is replaced by Met, completely lost the kinase activity. We therefore generated an expression plasmid encoding FLAG-Plk1(K82M), and then examined whether Plk1(K82M) could associate with p53, and also affect the p53-mediated transcriptional activation. Immunoprecipitation followed by Western detection of endogenous p53 indicated that p53 interacted with both the wild-type Plk1 and the kinase-deficient Plk1(K82M) (Fig. 9*A*). The effects of the lysine mutation on the p53-mediated transcriptional activation were tested by luciferase reporter analysis. In contrast to the wild-type Plk1, the kinase-deficient Plk1(K82M) failed to reduce the p53-mediated reporter expression driven by those constructs (Fig. 9, *B–D*).

To examine the effect of Plk1(K82M) on p53-dependent apoptosis, H1299 cells were transfected with the expression plasmid for p53 along with or without the expression plasmid for FLAG-Plk1(K82M). Forty-eight hours after transfection, their viability was measured by cell survival assay. As expected, the p53-dependent decrease in the number of viable cells was unaffected in the presence of the exogenous FLAG-Plk1(K82M) (Fig. 9*E*). Taken together, our results strongly suggest that the kinase activity of Plk1 is required for Plk1-dependent inhibition of p53.

ATM Antagonizes the Inhibitory Effect of Plk1 on p53—Plk1 kinase activity has been shown to be inhibited in an ATM-dependent manner in response to DNA damage (19, 20). The kinase activity of ATM was significantly increased after DNA damage, and ATM was able to phosphorylate p53 at the NH_2 terminus on serine 15 to enhance its stability as well as its transactivation activity (48–50). To examine whether ATM could affect the Plk1-mediated inhibition of p53, we transiently co-transfected H1299 cells with expression plasmids for p53 and FLAG-Plk1 together with or without increasing amounts of ATM expression plasmid, and the ability of p53 to drive transcription from the $p21^{WAF1}$ reporter was measured. As expected, co-expression of p53 with ATM resulted in an increase in the transcriptional activity of p53 as compared with that of cells expressing p53 alone (Fig. 10). Increasing amounts of ATM largely abrogated the Plk1-mediated inhibition of the p53-dependent transcriptional activation. It thus appears that ATM could inhibit the activity of Plk1 and thereby restore the transcriptional activity of p53.

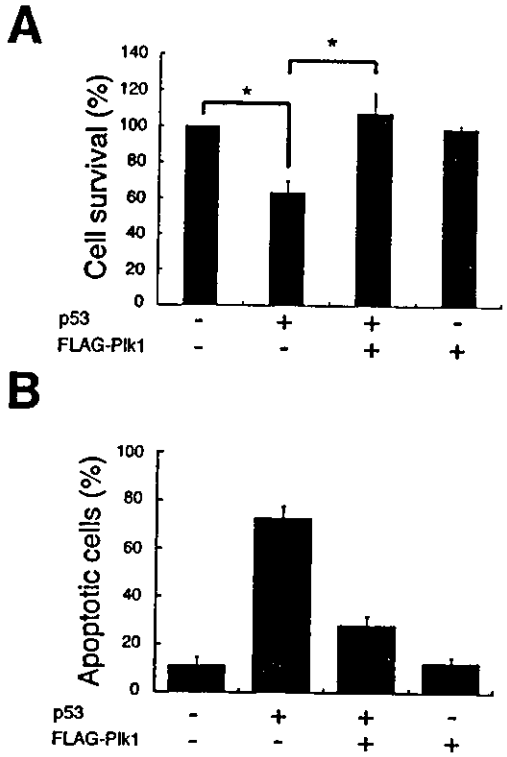

FIG. 8. **Plk1 inhibits the pro-apoptotic activity of p53.** *A*, H1299 cells were transiently co-transfected with 0.6 μg of the expression plasmid for p53 together with or without 1.2 μg of the FLAG-Plk1 expression plasmid. The total amount of plasmid DNA was kept constant (2 μg) with the empty plasmid. At 48 h after transfection, cell viability was determined by MTT cell survival assays. The graph (mean ± S.D. of three independent experiments) represents relative viability based on the percent of viable cells compared with the control transfection (pcDNA3). The percentage of viable cells expressing p53 alone is significantly different from that of viable cells expressing p53 and FLAG-Plk1 ($p < 0.0001$). *B*, H1299 cells were transiently co-transfected with the indicated combinations of the expression plasmids. A constant amount of the GFP expression plasmid (200 ng) was included in all combinations, and the total amount of plasmid DNA was kept constant (2 μg) by including an appropriate amount of empty plasmid. Forty-eight hours after transfection, transfected cells were identified by the presence of green fluorescence. Cell nucleus was stained with propidium iodide to reveal nuclear condensation and fragmentation. The number of GFP-positive cells with condensed and fragmented nuclei was scored, and the percentage of apoptotic cells shown in each column represents the mean of three independent experiments.

DISCUSSION

In the present study, we have found that Plk1 interacts with p53 and inhibits its transactivation as well as apoptosis-inducing activity in mammalian cultured cells. This interaction is mediated by the sequence-specific DNA-binding domain of p53 and the region of Plk1 containing the kinase domain. Importantly, Plk1-mediated inhibition of p53 requires its kinase activity and is attenuated with ATM. Thus, our present data support the hypothesis that p53 is one of the critical targets of Plk1, and that Plk1-mediated inhibition of p53 contributes at least in part to cell fate decisions regarding survival and tumorigenesis.

The expression of *Plk1* was significantly down-regulated in response to cisplatin treatment. Recently, Ree *et al.* (51) found that ionizing radiation leads to the suppression of *Plk1* mRNA expression. It is of interest to examine whether genotoxic stresses other than cisplatin and ionizing radiation could also repress the expression of *Plk1*. On the other hand, *Plk1* mRNA expression is significantly induced in various human primary tumors (27). It is necessary to identify the promoter region as well as the transcription factor(s) required for the transcriptional regulation of *Plk1* in cancerous cells. In good agreement with the previous observations (52), Uchiumi *et al.* (53) have identified the regulatory regions responsible for the activation of the human *Plk1* promoter, which include a consensus Sp1-binding site and a CCAAT box. It has been shown that the transcription factor NF-Y, a heterotrimeric complex consisting of NF-YA, NF-YB, and NF-YC, recognizes and binds to the CCAAT box (54). Indeed, the electrophoretic mobility shift assay revealed that NF-Y binds to the CCAAT box present within the human *Plk1* promoter region, however, it remains to be determined whether NF-Y and/or Sp1 could actually transactivate the *Plk1* promoter in tumor cells (53). Recently, Lee and Pedersen (55) have reported that there exist 6 GC boxes and the CCAAT box within the *type II hexokinase* (*HKII*) promoter, and that NF-Y and Sp family members including Sp1 might contribute to up-regulation of the *HKII* gene in tumor cells. Further studies regarding the transcriptional regulation of the *Plk1* gene are necessary to clarify the molecular mechanisms of Plk1-dependent tumorigenesis.

During the DNA damage response, the activity of ATM is significantly increased and is responsible for the rapid phosphorylation of p53 at Ser^{15} (48–50). This ATM-dependent phosphorylation contributes to the increased stability and activity of p53 by facilitating its dissociation from MDM2 (56). In addition, phosphorylation of p53 at Ser^{15} induces its binding to the transcriptional co-activator p300 (57). Recently, it has been shown that Plk1 activity is inhibited in response to DNA damage, and this inhibition occurs in an ATM-dependent manner (19, 20). Our present data demonstrate that the Plk1-mediated inhibition of p53 activity is rescued by the co-expression of ATM, suggesting that, in addition to the ATM-dependent phosphorylation of p53, the activity of p53 may be enhanced at least in part by the ATM-dependent inhibition of Plk1. Intriguingly, Liu and Erikson (33) reported that p53 is significantly stabilized in Plk1-depleted cells. In accordance with their findings, we have shown that the exposure of SH-SY5Y cells to cisplatin leads to a remarkable accumulation of p53, which is strongly associated with a significant down-regulation of the endogenous Plk1 both at mRNA and protein levels, suggesting that Plk1 is closely involved in the regulation of p53 stability and thereby modulates its activity. Under our experimental conditions, however, overexpression of FLAG-Plk1 did not affect the amounts of the endogenous as well as the ectopically expressed p53.

The pro-apoptotic function of p53 involves its ability to act as a transcription factor in transactivating downstream target gene promoters. The majority of missense mutations of p53 detected in human tumors occur within its sequence-specific DNA-binding domain, and these mutations cause the loss of p53 activity (58). Thus, the structural integrity of this domain is required for p53 function. On the other hand, several viral and cellular proteins inactivate p53 through a variety of different mechanisms (58). MDM2 and Pirh2 promote ubiquitination and degradation of p53 (59–62). Sir2α interacts with p53 and induces its deacetylation (63). In addition, S100B calcium-binding protein prevents the oligomerization of p53 to inhibit its function (64). Based on our systematic immunoprecipitation analysis, Plk1 binds to p53 through the sequence-specific DNA-binding domain of p53. Intriguingly, SV40 large T antigen binds to the sequence-specific DNA-binding domain of p53, and abrogates DNA binding as well as the transactivation function of p53 (65, 66). It is thus likely that, like SV40 large T antigen, Plk1 might mask this domain of p53 by direct binding, and thereby inhibit its sequence-specific transcriptional activity. Further study is required to identify the detailed molecular mechanism.

In sharp contrast to Plk1, Xie *et al.* (26) found that the kinase

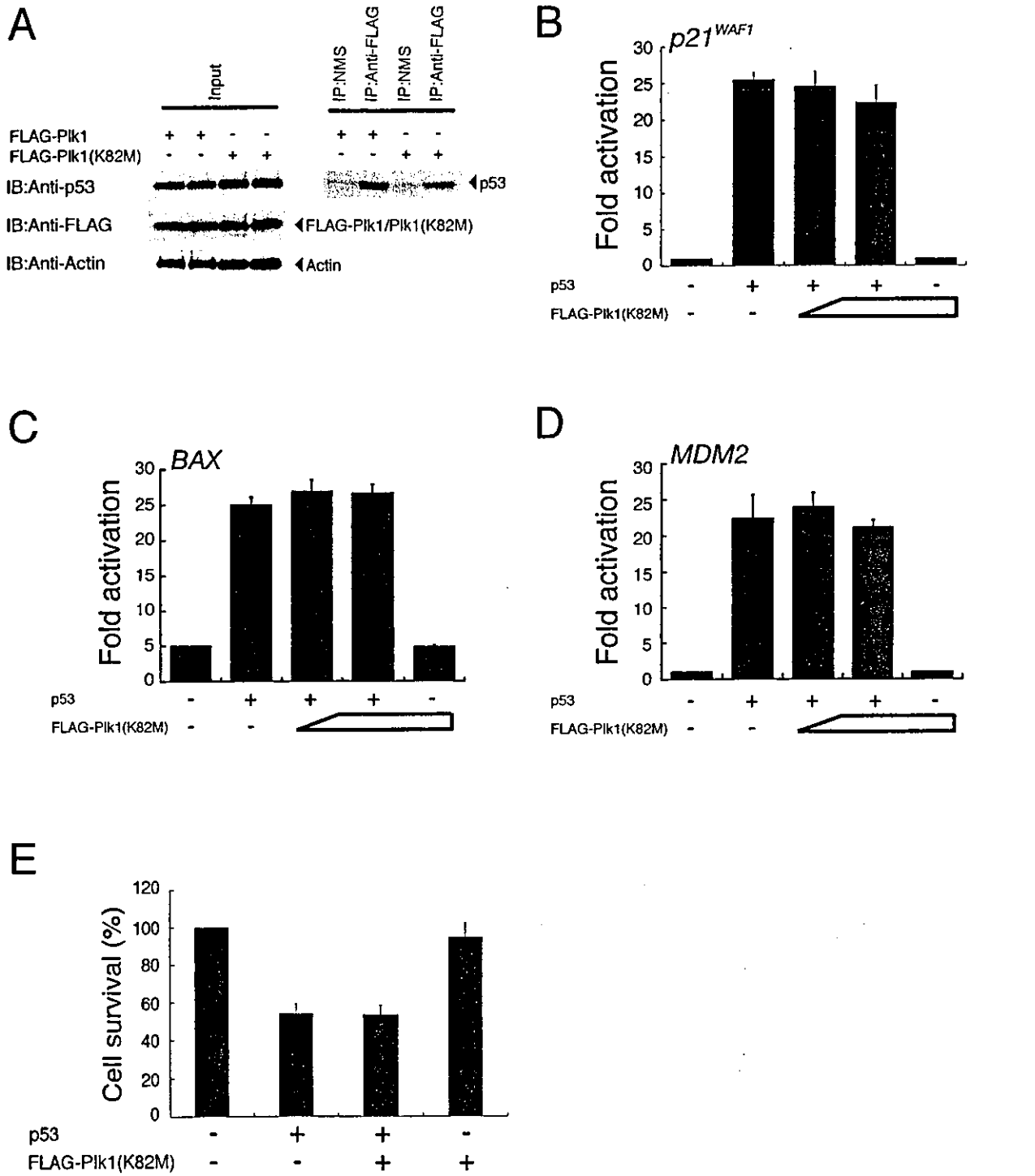

FIG. 9. **Kinase-deficient Plk1(K82M) fails to reduce the activity of p53.** *A*, Plk1(K82M) retains an ability to interact with p53. COS7 cells were transiently transfected with the expression plasmid for FLAG-Plk1 or FLAG-Plk1(K82M). Forty-eight hours after transfection, cell lysates were prepared and subjected to anti-FLAG immunoprecipitation followed by immunoblotting with monoclonal anti-p53 antibody. Immunoprecipitation with NMS was used as a negative control. Equal amounts of protein derived from cell lysates were immunoblotted with monoclonal anti-p53, monoclonal anti-FLAG, or with polyclonal anti-actin antibody. *B–D*, Plk1(K82M) has an undetectable effect on the transcriptional activity of p53. H1299 cells were transiently co-transfected with a fixed amount of the p53 expression plasmid (25 ng) and the p53-responsive luciferase reporter construct carrying the $p21^{WAF1}$ (*B*), *BAX* (*C*), or *MDM2* (*D*) promoter (100 ng) in the presence or absence of increasing amounts of the expression plasmid encoding FLAG-Plk1(K82M) (100 or 200 ng). The total amount of plasmid DNA per transfection was kept constant (510 ng) with pcDNA3. Determination and calculation of the luciferase activities are described in the legend to Fig. 6. *E*, Plk1(K82M) is unable to inhibit the pro-apoptotic function of p53. H1299 cells were transiently co-transfected with the p53 expression plasmid (0.6 μg) together with or without the expression plasmid for FLAG-Plk1(K82M) (1.2 μg). Forty-eight hours after transfection, their viability was measured by MTT cell survival assays as described in the legend to Fig. 8.

activity of Plk3 is rapidly enhanced in response to DNA damage in an ATM-dependent fashion. They also described that Plk3 has the ability to interact directly with p53 and phosphorylate p53 at Ser^{20}. Moreover, a kinase-defective mutant form of Plk3 fails to phosphorylate p53, and abrogates the p53-mediated transcriptional activation as well as growth suppression, indicating that Plk3 might enhance the p53 activity through Ser^{20} phosphorylation of p53 (26). In addition to Ser^{15} phosphoryla-

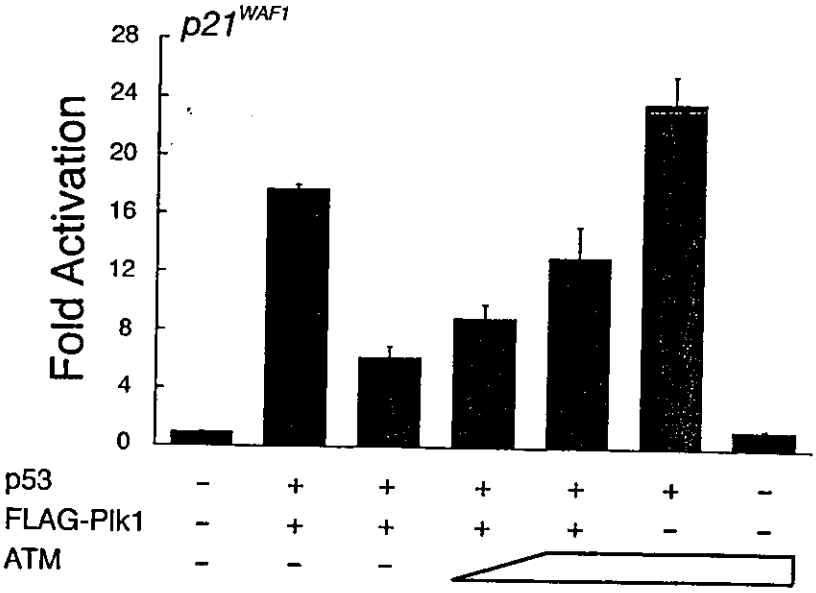

FIG. 10. **ATM antagonizes the inhibitory effect of Plk1 on the p53-dependent transactivation.** H1299 cells were transiently co-transfected with the expression plasmids encoding p53 (25 ng) and FLAG-Plk1 (200 ng) along with the luciferase reporter construct containing the p53-responsive element from the $p21^{WAF1}$ promoter in the presence or absence of increasing amounts of ATM expression plasmid (50 or 100 ng). pcDNA3 was used to equalize the amount of plasmid in each transfection, and the *Renilla* luciferase plasmid was included in the transfection mixture to normalize the transfection efficiency. Determination and calculation of the luciferase activities are described in the legend to Fig. 6.

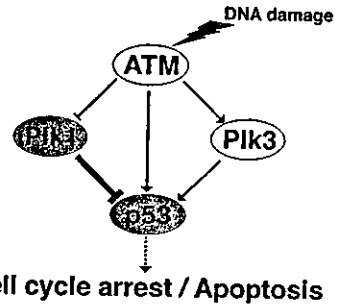

FIG. 11. **Schematic representation of interactions among ATM, Plk1, Plk3, and p53 in response to DNA damage.**

tion of p53, DNA damage-induced phosphorylation of p53 at Ser^{20} prevents its association with MDM2 and results in its stabilization (67). Of note, it has been shown that Plk1 phosphorylates p53 *in vitro* but on residues that might be different from that mediated by Plk3 (26). According to their phosphopeptide mapping analysis, at least three unique radiolabeled tryptic peptides derived from recombinant p53 were detected in the presence of Plk1. Recently, Nakajima *et al.* (68) identified a sequence (D/E)*X*(S/T)ψ*X*(D/E) (*X*, any amino acid; ψ, a hydrophobic amino acid) as a consensus motif for Plk1-dependent phosphorylation (68). During the search for a putative phosphorylation site(s) targeted by Plk1 within the amino acid sequence of p53, we found a related motif (^{254}IITLED^{259}) present within the sequence-specific DNA-binding domain of p53, suggesting that this motif could be one of the putative phosphorylation sites of p53 targeted by Plk1, although there is no direct evidence for this possibility. According to our present results, the kinase-deficient mutant form of Plk1 that retained an ability to associate with p53, failed to reduce the transcriptional as well as apoptosis-inducing activity of p53, suggesting that the kinase activity of Plk1 is critical for the Plk1-dependent inhibition of p53. Thus, identification of the major phosphorylation site(s) of p53 by Plk1 is required to establish the functional significance of the Plk1-mediated phosphorylation of p53. In contrast, Liu and Erikson (33) reported that, like wild-type mouse Plk1, co-expression of the kinase-defective (K82M) mouse Plk1 partially rescued the apoptotic phenotype induced by the depletion of Plk1, indicating that the kinase activity is not necessary for its anti-apoptotic activity. They also described that their kinase-defective mouse Plk1 has 15–20% of wild-type kinase activity, raising a possibility that the residual kinase activity of their mouse Plk1(K82M) might be enough to inhibit the Plk1 depletion-induced apoptosis.

Fig. 11 shows a model that incorporates our present findings, and illustrates various interactions in response to DNA damage. Given the fact that the differential expression of Plk1 and Plk3 during the cisplatin-induced apoptosis, and their differential effects on p53, it is conceivable that the balance between intracellular expression levels of Plk1 with oncogenic potential and pro-apoptotic Plk3 is at least in part responsible for the determination of the cell fate via the physical and functional interaction with p53.

Acknowledgments—We are grateful to Dr. Y. Shiloh and the Japanese Study Group for Pediatric Liver Tumor for kindly providing the ATM expression plasmid and hepatoblastoma tissues, respectively. We thank Dr. S. Sakiyama and members of our laboratory for helpful discussions. We also thank Y. Nakamura and M. Kikawa for excellent technical assistance.

REFERENCES

1. Glover, D. M., Hagan, I. M., and Tavares, A. A. (1998) *Genes Dev.* **12**, 3777–3787
2. Clay, F. J., McEwen, S. J., Bertoncello, I., Wilks, A. F., and Dunn, A. R. (1993) *Proc. Natl. Acad. Sci. U. S. A.* **90**, 4882–4886
3. Lee, K. S., Grenfell, T. Z., Yarm, F. R., and Erikson, R. L. (1998) *Proc. Natl. Acad. Sci. U. S. A.* **95**, 9301–9306
4. Song, S., Grenfell, T., Garfield, S., Erikson, R. L., and Lee, K. S. (2000) *Mol. Cell. Biol.* **20**, 286–298
5. Jang, Y.-J., Lin, C.-Y., Ma, S., and Erikson, R. L. (2002) *Proc. Natl. Acad. Sci. U. S. A.* **99**, 1984–1989
6. Glover, D. M., Ohkura, H., and Tavares, A. (1996) *J. Cell Biol.* **135**, 1681–1684
7. Lane, H., and Nigg, E. A. (1997) *Trends Cell. Biol.* **7**, 63–68
8. Nigg, E. A. (1998) *Curr. Opin. Cell Biol.* **10**, 776–783
9. Hamanaka, R., Maloid, S., Smith, M. R., O'Connell, C. D., Longo, D. L., and Ferris, D. K. (1994) *Cell Growth & Differ.* **5**, 249–257
10. Smith, M. R., Wilson, M. L., Hamanaka, R., Chase, D., Kung, H.-F., Longo, D. L., and Ferris, D. K. (1997) *Biochem. Biophys. Res. Commun.* **234**, 397–405
11. Lake, R. J., and Jelinek, W. R. (1993) *Mol. Cell. Biol.* **13**, 7793–7801
12. Golsteyn, R. M., Schultz, S. J., Bartek, J., Ziemiecki, A., Ried, T., and Nigg, E. A. (1994) *J. Cell Sci.* **107**, 1509–1517
13. Holtrich, U., Wolf, G., Brauninger, A., Karn, T., Bohme, B., Rubsamen-Waigmann, H., and Strebhardt, K. (1994) *Proc. Natl. Acad. Sci. U. S. A.* **91**, 1736–1740
14. Simmons, D. L., Neel, B. G., Stevens, R., Evett, G., and Erikson, R. L. (1992) *Mol. Cell. Biol.* **12**, 4164–4169
15. Donohue, P. J., Alberts, G. F., Guo, Y., and Winkles, J. A. (1995) *J. Biol. Chem.* **270**, 10351–10357
16. Golsteyn, R. M., Mundt, K. E., Fry, A. M., and Nigg, E. A. (1995) *J. Cell Biol.* **129**, 1617–1628
17. Hamanaka, R., Smith, M. R., O'Connor, P. M., Maloid, S., Mihalic, K., Spivak, J. L., Longo, D. L., and Ferris, D. K. (1995) *J. Biol. Chem.* **270**, 21086–21091
18. Qian, Y.-W., Erikson, E., and Maller, J. L. (1998) *Science* **282**, 1701–1704
19. Smits, V. A., Klompmaker, R., Arnaud, L., Rijksen, G., Nigg, E. A., and Medema, R. H. (2000) *Nat. Cell Biol.* **2**, 672–676
20. van Vugt, M. A. T. M., Smits, V. A. J., Klompmaker, R., and Medema, R. H. (2001) *J. Biol. Chem.* **276**, 41656–41660
21. Toyoshima-Morimoto, F., Taniguchi, E., Shinya, N., Iwamatsu, A., and

Nishida, E. (2001) *Nature* **410,** 215–220
22. Yuan, J., Eckerdt, F., Bereiter-Hahn, J., Kurunci-Csacsko, E., Kaufmann, M., and Strebhardt, K. (2002) *Oncogene* **21,** 8282–8292
23. Toyoshima-Morimoto, F., Taniguchi, E., and Nishida, E. (2002) *EMBO Rep.* **3,** 341–348
24. Ouyang, B., Pan, H., Lu, L., Li, J., Stambrook, P., Li, B., and Dai, W. (1997) *J. Biol. Chem.* **272,** 28646–28651
25. Bahassi, E. M., Conn, C. W., Myer, D. L., Hennigan, R. F., McGowan, C. H., Sanchez, Y., and Stambrook, P. J. (2002) *Oncogene* **21,** 6633–6640
26. Xie, S., Wu, H., Wang, Q., Cogswell, J. P., Husain, I., Conn, C., Stambrook, P., Jhanwar-Uniyal, M., and Dai, W. (2001) *J. Biol. Chem.* **276,** 43305–43312
27. Yuan, J., Horlin, A., Hock, B., Stutte, H. J., Rubsamen-Waigmann, H., and Strebhardt, K. (1997) *Am. J. Pathol.* **150,** 1165–1172
28. Wolf, G., Elez, R., Doermer, A., Holtrich, U., Ackermann, H., Stutte, H. J., Altmannsberger, H. M., Rubsamen-Waigmann, H., and Strebhardt, K. (1997) *Oncogene* **14,** 543–549
29. Knecht, R., Elez, R., Oechler, M., Solbach, C., von Ilberg, C., and Strebhardt, K. (1999) *Cancer Res.* **59,** 2794–2797
30. Knecht, R., Oberhauser, C., and Strebhardt, K. (2000) *Int. J. Cancer* **89,** 535–536
31. Spankuch-Schmitt, B., Wolf, G., Solbach, C., Loibl, S., Knecht, R., Stegmuller, M., von Minckwitz, G., Kaufmann, M., and Strebhardt, K. (2002) *Oncogene* **21,** 3162–3171
32. Spankuch-Schmitt, B., Bereiter-Hahn, J., Kaufmann, M., and Strebhardt, K. (2002) *J. Natl. Cancer Inst.* **94,** 1863–1877
33. Liu, X., and Erikson, R. L. (2003) *Proc. Natl. Acad. Sci. U. S. A.* **100,** 5789–5794
34. Li, B., Ouyang, B., Pan, H., Reissmann, P. T., Slamon, D. J., Arceci, R., Lu, L., and Dai, W. (1996) *J. Biol. Chem.* **271,** 19402–19408
35. Dai, W., Li, Y., Ouyang, B., Pan, H., Reissmann, P., Li, J., Wiest, J., Stambrook, P., Gluckman, J. L., Noffsinger, A., and Bejarano, P. (2000) *Genes Chromosomes Cancer* **27,** 332–336
36. Conn, C. W., Hennigan, R. F., Dai, W., Sanchez, Y., and Stambrook, P. J. (2000) *Cancer Res.* **60,** 6826–6831
37. Xie, S., Wang, Q., Wu, H., Cogswell, J., Lu, L., Jhanwar-Uniyal, M., and Dai, W. (2001) *J. Biol. Chem.* **276,** 36194–36199
38. Nakamura, Y., Ozaki, T., Nakagawara, A., and Sakiyama, S. (1997) *Eur. J. Cancer* **33,** 1986–1990
39. Nakagawa, T., Takahashi, M., Ozaki, T., Watanabe, K., Todo, S., Mizuguchi, H., Hayakawa, T., and Nakagawara, A. (2002) *Mol. Cell. Biol.* **22,** 2575–2585
40. Watanabe, K., Ozaki, T., Nakagawa, T., Miyazaki, K., Takahashi, M., Hosoda, M., Hayashi, S., Todo, S., and Nakagawara, A. (2002) *J. Biol. Chem.* **277,** 15113–15123
41. Kim, E.-J., Park, J.-S., and Um, S.-J. (2002) *J. Biol. Chem.* **277,** 32020–32028
42. Taniguchi, E., Totoshima-Morimoto, F., and Nishida, E. (2002) *J. Biol. Chem.* **277,** 48884–48888
43. Kastan, M. B., Zhan, Q., el-Deiry, W. S., Carrier, F., Jacks, T., Walsh, W. V., Plunkett, B. S., Vogelstein, B., and Fornace, A. J., Jr. (1992) *Cell* **71,** 587–597
44. Shaulsky, G., Goldfinger, N., Ben-Ze'ev, A., and Rotter, V. (1990) *Mol. Cell. Biol.* **10,** 6565–6577
45. Dang, C. V., and Lee, W. M. (1989) *J. Biol. Chem.* **264,** 18019–18023
46. Zaika, A. I., Slade, N., Erster, S. H., Sansome, C., Joseph, T. W., Pearl, M., Chalas, E., and Moll, U. M. (2002) *J. Exp. Med.* **196,** 765–780
47. Zeng, X., Chen, L., Jost, C. A., Maya, R., Keller, D., Wang, X., Kaelin, W. G., Oren, M., Chen, J., and Lu, H. (1999) *Mol. Cell. Biol.* **19,** 3257–3266
48. Banin, S., Moyal, L., Shieh, S., Taya, Y., Anderson, C. W., Chessa, L., Smorodinsky, N. I., Prives, C., Reiss, Y., Shiloh, Y., and Ziv, Y. (1998) *Science* **281,** 1674–1677
49. Canman, C. E., Lim, D. S., Cimprich, K. A., Taya, Y., Tamai, K., Sakaguchi, K., Appella, E., Kastan, M. B., and Siliciano, J. D. (1998) *Science* **281,** 1677–1679
50. Khanna, K. K., Keating, K. E., Kozlov, S., Scott, S., Gatei, M., Hobson, K., Taya, Y., Gabrielli, B., Chan, D., Lees Miller, S. P., and Lavin, M. F. (1998) *Nat. Genet.* **20,** 398–400
51. Ree, A. H., Bratland, A., Nome, R. V., Stokke, T., and Fodstad, O. (2003) *Oncogene* **22,** 8952–8955
52. Brauninger, A., Strebhardt, K., and Rubsamen-Waigmann, H. (1995) *Oncogene* **11,** 1793–1800
53. Uchiumi, T., Longo, D. L., and Ferris, D. K. (1997) *J. Biol. Chem.* **272,** 9166–9174
54. Mantovani, R. (1999) *Gene (Amst.)* **239,** 15–27
55. Lee, M. G., and Pedersen, P. L. (2003) *J. Biol. Chem.* **278,** 41047–41058
56. Shieh, S. Y., Ikeda, M., Taya, Y., and Prives, C. (1997) *Cell* **91,** 325–334
57. Lambert, P. F., Kashanchi, F., Radonovich, M. F., Shiekhattar, R., and Brady, J. N. (1998) *J. Biol. Chem.* **273,** 33048–33053
58. Prives, C., and Hall, P. A. (1999) *J. Pathol.* **187,** 112–126
59. Haupt, Y., Maya, R., Kazaz, A., and Oren, M. (1997) *Nature* **387,** 296–299
60. Kubbutat, M. H. G., Jones, S. N., and Vousden, K. H. (1997) *Nature* **387,** 299–303
61. Honda, R., Tanaka, H., and Yasuda, Y. (1997) *FEBS Lett.* **420,** 25–27
62. Leng, R. P., Lin, Y., Ma, W., Wu, H., Lemmers, B., Chung, S., Parant, J. M., Lozano, G., Hakem, R., and Benchimol, S. (2003) *Cell* **112,** 779–791
63. Luo, J., Nikolaev, A. Y., Imai, S., Chen, D., Su, F., Shiloh, A., Guarente, L., and Gu, W. (2001) *Cell* **107,** 137–148
64. Lin, J., Blake, M., Tang, C., Zimmer, D., Rustandi, R. R., Weber, D. J., and Carrier, F. (2001) *J. Biol. Chem.* **276,** 35037–35041
65. Tan, T.-H., Wallis, J., and Levine, A. J. (1986) *J. Virol.* **59,** 574–583
66. Farmer, G., Bargonetti, J., Zhu, H., Friedman, P., Prywes, R., and Prives, C. (1992) *Nature* **358,** 83–86
67. Vousden, K. H. (2002) *Biochim. Biophys. Acta* **1602,** 47–59
68. Nakajima, H., Toyoshima-Morimoto, F., Taniguchi, E., and Nishida, E. (2003) *J. Biol. Chem.* **278,** 25277–25280

Int. J. Cancer: 112, 365–375 (2004)

Publication of the International Union Against Cancer

LOW EXPRESSION OF HUMAN TUBULIN TYROSINE LIGASE AND SUPPRESSED TUBULIN TYROSINATION/DETYROSINATION CYCLE ARE ASSOCIATED WITH IMPAIRED NEURONAL DIFFERENTIATION IN NEUROBLASTOMAS WITH POOR PROGNOSIS

Chiaki KATO[1,2], Kou MIYAZAKI[1], Atsuko NAKAGAWA[3], Miki OHIRA[1], Yohko NAKAMURA[1], Toshinori OZAKI[1], Toshio IMAI[2] and Akira NAKAGAWARA[1]*

[1]*Division of Biochemistry, Chiba Cancer Center Research Institute, Chiba, Japan*
[2]*Department of Physiologic Chemistry Faculty of Science, Toho University, Chiba, Japan*
[3]*Second Department of Pathology, Aichi Medical University, Nagakute, Japan*

Neuroblastoma (NBL), one of the most common childhood solid tumors, has a distinct nature in different prognostic subgroups. However, the precise mechanism underlying this phenomenon remains largely unknown. To understand the molecular and genetic bases of neuroblastoma, we have generated its cDNA libraries and identified a human ortholog of *tubulin tyrosine ligase* gene (*hTTLNbla0660*) as a differentially expressed gene at high levels in a favorable subset of the tumor. Tubulin is subjected to several types of evolutionarily conserved posttranslational modification, including tyrosination and detyrosination. Tubulin tyrosine ligase catalyzes ligation of the tyrosine residue to the COOH terminus of the detyrosinated form of α-tubulin. The measurement of *hTTL* mRNA expression in 74 primary neuroblastomas by quantitative real-time reverse transcription-PCR revealed that its high expression was significantly associated with favorable stages (1, 2 and 4s; $p = 0.0069$), high *TrkA* expression ($p = 0.002$), a single copy of *MYCN* ($p < 0.00005$), tumors found by mass screening ($p = 0.0042$), nonadrenal origin ($p = 0.0042$) and good prognosis ($p = 0.023$). The log-rank test showed that high expression of *hTTL* was an indicator of favorable prognosis ($p = 0.026$). Immunohistochemical analysis using specific antibodies generated by us demonstrated that tyrosinated tubulin (Tyr-tubulin), detyrosinated tubulin (Glu-tubulin) and hTTL as well as Δ2-tubulin were positive in favorable tumors, whereas only Δ2-tubulin was positive in the tumors with *MYCN* amplification. In an RTBM1 neuroblastoma cell line, hTTL was increased after treating the cells with bone morphogenetic protein 2 (BMP2) or all-trans retinoic acid (RA), which induced neuronal differentiation. These results suggest that the deregulated tubulin tyrosination/detyrosination cycle caused by decreased expression of hTTL is associated with inhibition of neuronal differentiation and enhancement of cell growth in the primary neuroblastomas with poor outcome.

Key words: *tubulin tyrosine ligase; tubulin tyrosination; neuroblastoma; neuronal differentiation; prognostic factor*

Tubulin is one of the most important molecular components that regulate cytoskeletal structure relating to cell motility, cell division, differentiation, invasion and metastasis in cancer. However, functional modification of tubulin protein has still been elusive. Tubulin is subjected to several types of evolutionarily conserved posttranslational modification that includes tyrosination/detyrosination, acetylation, phosophorylation, palmitoylation, polyglutamylation and polyglycylation.[1–4] The discovery of tyrosination cycle stems from the serial observations that the addition of radiolabeled tyrosine to a rat brain cytosolic extract leads to tyrosination of the COOH terminus of a single endogenous protein, α-tubulin, by a translation-independent mechanism.[5–7] Posttranslational incorporation of tyrosine into the tubulin has also been shown to occur *in vivo*.[8–10] The cycle of tyrosination/detyrosination is evolutionarily conserved[11–13] and is regulated by both tubulin tyrosine ligase (TTL) and carboxypeptidase, the gene of which has not yet been identified (Fig. 1). Microtubule dynamics is also an important factor. TTL protein was first purified by immunoaffinity chromatography from the lysates of bovine and porcine brains and was extensively characterized by protein sequencing.[14] Recently, rat *TTL* cDNA has also been isolated.[15] Interestingly, in 1991, Paturle-Lafanechere *et al.*[16] identified a nontyrosinatable variant of tubulin that lacked 2 amino acid residues, glutamic acid and tyrosine, at the COOH terminus (Δ2-tubulin). Δ2-tubulin was found to accumulate in mature neurons and in stable microtubule assemblies in cells.[17,18] In some tumors, it also accumulated in the cellular cytoplasm in association with decreased levels of TTL, suggesting that the amount of Δ2-tubulin and TTL expression level in tumor cells are important to define the malignant grade of cancer.[19] However, pathophysiologic significance of the tyrosination/detyrosination cycle in normal and cancer cells still remains unclear.

Neuroblastoma (NBL) is one of the most common childhood solid tumors and has distinct biologic characteristics in different prognostic subgroups. For example, NBL in patients under 1 year of age usually regresses spontaneously, whereas that in patients over 1 year of age often grows aggressively and eventually kills the patient. To understand the molecular mechanism of distinct biology and tumorigenesis of NBL, we have previously performed a comprehensive approach to unveil the gene expression profiles among the NBL subsets.[20,21] We constructed the subset-specific oligo-capping cDNA libraries from the primary NBL tissues with favorable (stage 1, high expression of *TrkA* and a single copy of *MYCN*) and unfavorable (stage 3 or 4, decreased expression of *TrkA* and *MYCN* amplification) characteristics and randomly cloned 4,654 cDNAs. After adding the cDNAs obtained from the stage 4s NBL cDNA library to our NBL gene collection, we made an in-house cDNA microarray carrying 5,340 genes proper to NBL. The comprehensive analysis of 136 NBLs using the microar-

Abbreviations: BMP2, bone morphogenetic protein 2; DMEM, Dulbecco's modified Eagle's medium; ECL, enhanced chemiluminescence; FBS, fetal bovine serum; hTTL, human tubulin tyrosine ligase; NBL, neuroblastoma; RA, retinoic acid; TCP, tubulin carboxypeptidase; TTL, tubulin tyrosine ligase.

Grant sponsor: Grant-in-Aid for Scientific Research and for Scientific Research on Priority Areas, Medical Genome Science from the Ministry of Education, Science, Sports and Culture, Japan; Grant sponsor: Hisamitsu Pharmaceutical Co. Inc.

*Correspondence to: Division of Biochemistry, Chiba Cancer Center Research Institute, 666-2 Nitona, Chuoh-ku, Chiba 260-8717, Japan. Fax: +81-43-265-4459. E-mail: akiranak@chiba-ccri.chuo.chiba.jp

Received 27 January 2004; Accepted 15 April 2004

DOI 10.1002/ijc.20431
Published online 23 June 2004 in Wiley InterScience (www.interscience.wiley.com).

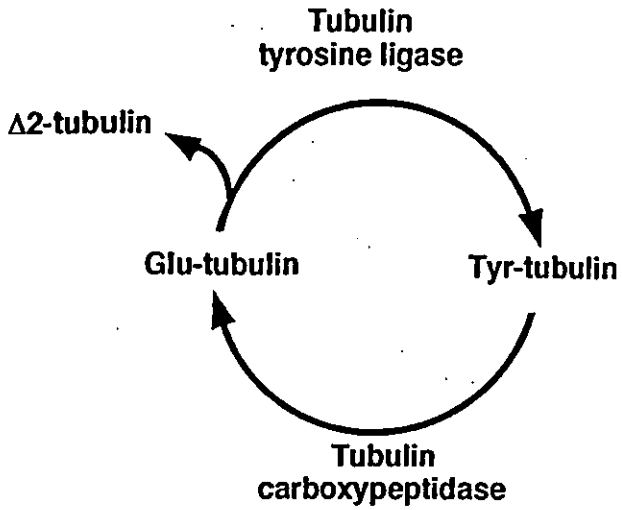

FIGURE 1 – The tyrosination/detyrosination cycle catalyzed by tubulin tyrosine ligase and tubulin carboxypeptidase.

ray showed that many genes that are related to the cytoskeletal components, including α-tubulin, had prognostic significance (data not shown).

In the present study, we have cloned for the first time the human ortholog of TTL (*hTTL*) from both the NBL and a fetal brain cDNA libraries. The analysis using 74 primary NBLs shows that expression of *hTTL* mRNA is significantly lower in unfavorable NBLs than in favorable tumors. The examination using specific antibodies raised against hTTL, Tyr-tubulin, Glu-tubulin and Δ2-tubulin demonstrates that hTTL is increased during induction of neuronal differentiation of cultured NBL cells treated with BMP2 or RA. The immunohistochemical study shows that hTTL, Tyr-tubulin, Glu-tubulin and Δ2-tubulin are positive in favorable NBLs, whereas only Δ2-tubulin is positive in aggressive NBLs with *MYCN* amplification. These suggested that the tyrosination/detyrosination cycle of α-tubulin is active in NBLs with high potential to differentiate or undergo apoptosis, while it is disregulated by downregulation of hTTL in *MYCN*-amplified NBLs, resulting in accumulation of Δ2-tubulin.

MATERIAL AND METHODS

Tumor specimen

Fresh frozen tumor tissues obtained by surgery or biopsy were sent to the Division of Biochemistry, Chiba Cancer Center Research Institute, from various hospitals in Japan with informed consent. Ninety tumors examined in this study were staged according to the International Neuroblastoma Staging System (INSS).[22] The number of tumors subjected to quantitative real-time RT-PCR were 24 in stage 1, 11 in stage 2, 5 in stage 4s, 10 in stage 3 and 24 in stage 4. The patients were treated according to the protocols previously described.[23] Biologic information on each tumor, including *MYCN* gene copy number, *TrkA* gene expression and DNA ploidy, was analyzed in our laboratory as described previously.[24]

Cell culture and transfection

COS7 and HEK293T cells were maintained in Dulbecco's modified Eagle's medium (DMEM) supplemented with 10% heat-inactivated fetal bovine serum (FBS; Life Technologies, Gaithersburg, MD) and penicillin (100 IU/ml)/streptomycin (100 μg/ml). Human neuroblastoma RTBM1 cells were grown in RPMI-1640 medium containing 10% heat-inactivated FBS and antibiotic mixture. Cultures were maintained at 37°C in a water-saturated atmosphere of 5% CO_2 in air. Transient transfection was performed by LipofectAMINE 2000 transfection reagent (Invitrogen, Carlsbad, CA) according to the manufacturer's instructions. In brief, cells were seeded in tissue culture plates to achieve 50% confluence. Twenty-four hours later, cells were transfected by using a mixture of the expression plasmids and LipofectAMINE 2000 transfection reagent in DMEM without serum. Forty-eight hours after transfection, cells were collected and analyzed by Western blotting. For neurite extension assays, RTBM1 cells were treated either with recombinant human BMP2 (Yamanouchi Pharmaceutical, Tokyo, Japan) or with RA at a final concentration of 1 nM or 5 μM, respectively.

RNA isolation and semiquantitative RT-PCR

Total RNA was prepared from neuroblastoma tissues according to the AGPC method.[25] Five micrograms of total RNA were subjected to the synthesis of the first-strand cDNA with $pd(N)_6$ random hexamer (Takara Shuzo, Otsu, Japan) and a Superscript II reverse transcriptase (Invitrogen) at 42°C for 90 min. The resultant cDNA was diluted to be a 1:20 solution and was amplified in a final volume of 10 μl of reaction mixture containing 100 μM of each deoxynucleoside triphosphate, 1 × PCR buffer, 1 μM of each primer and 0.2 U of rTaq DNA polymerase (Takara Bio, Ohtsu, Japan). The following primers were used: *hTTL*, 5′-CAGCTCTTCGGCTTTGACTT-3′ (sense) and 5′-GCTGTGGGCTGGATAAAGAG-3′ (antisense); human *GAPDH*, 5′-ACCTGACCTGCCGTCTAGAA-3′ (sense) and 5′-TCC ACCACCCTGTTGCTGTA-3′ (antisense). PCR templates were standardized by its *GAPDH* expression before performing semiquantitative PCR experiment. The PCR-amplified products were separated by electrophoresis on a 1.5% agarose gel and visualized by ethidium bromide poststaining.

Quantitative real-time RT-PCR

cDNA was prepared by the same method as in the semiquantitative RT-PCR and 2 μl of the 40-fold dilution was used for each PCR reaction. Primers and TaqMan probes for *hTTL* were designed using the primer design software Primer Express (Perkin-Elmer Applied Biosystems, Foster City, CA). The primer sequences for *hTTL* are 5′-AAGGAACTGCCTCCTGAGC-3′ and 5′-TCAATGAGCCAC ACCTTCA-3′. The probe sequence for *TTL* is 5′-FAM-ATTAGC ACCAAGCACCTCCCTTACCAGAGC-TAMRA-3′. PCR was carried out with the ABI Prism 7700 Sequence Detection System (Perkin-Elmer Applied Biosystems). Two μl of cDNA was amplified in a final volume of 25 μl containing 1 × TaqMan mixture, 300 nM each primer and 200 nM TaqMan probe. The thermal cycling condition was as follows: 50 cycles of a 2-step PCR (95°C for 15 sec, 60°C for 1 min) after the initial activation of UNG followed by denaturation (50°C for 2 min, 95°C for 10 min). TaqMan *GAPDH* control reagent kit (Roche Molecular Biochemicals, Basel, Switzerland) was used for the amplification of *GAPDH* according to the manufacturer's instructions; all data were normalized using *GAPDH* expression. The experiments were performed in triplicate for each data point.

Generation of polyclonal anti-hTTL antibodies

The polyclonal anti-hTTL antibody was raised in rabbits against Cys-coupled synthetic peptides derived from hTTL (222-RTASEPY-HVDNFQDKTCHLTNH-243 and 244-CIQKEYSKNYGKYEE-GNE-261). The polyclonal anti-Tyr-tubulin, anti-Glu-tubulin and anti-Δ2-tubulin antibodies were raised in rabbits immunized with Cys-coupled synthetic peptides corresponding to their COOH termini (CEEEGEEY, CGEEEGEE and CEGEEEGE, respectively). Antibodies were purified by using peptide-coupled affinity columns and tested for their ability to identify the corresponding proteins by Western blots. The synthetic peptides and antibodies were generated by Protein Express (Chiba, Japan).

Construction of FLAG-tagged hTTL expression plasmid

The FLAG-tagged hTTL expression plasmid was generated by PCR amplification using the cDNA library derived from human fetal brain (Stratagene, La Jolla, CA) and an *hTTL* cDNA that lacked the 5′-portion encoding the NH_2 terminal region of hTTL as templates. The forward and reverse primers used were 5′-TAAATAGTCGACGATATCATGGACTACAAGGACGAC

GACGACAAGTACACCTTCGTGGTACGCGATGAGAACAGC AGCGTCTACGCCGAGGTCTCCCGGCTGCTCCTCGCCA-3′ (sequence encoding FLAG epitope tag is in boldface, and *Eco*RV recognition site is underlined) and 5′-TACATGTCGACGCGG CCGCTCACAGCTTGAT GAA-3′ (*Not*I restriction site is underlined). The resulting PCR product was gel-purified, digested with *Eco*RV and *Not*I, inserted into identical restriction sites of a mammalian expression plasmid pIRESpuro2 (Clontech Laboratories, Palo Alto, CA) and its nucleotide sequence was verified by automated dideoxy terminator cycle sequencing.

Western blot analysis

Cells were washed in ice-cold phosphate-buffered saline (PBS), collected by centrifugation and lysed in 1 × sample buffer. Equal amounts of whole-cell lysates were fractionated by SDS-polyacrylamide gel electrophoresis (SDS-PAGE), and electrophoretically transferred onto a polyvinylidene difluoride (PVDF) membrane filter (Immobilon-P; Millipore, Billerica, MA). The filter was then blocked with Tris-buffered saline (TBS) containing 5% nonfat dry milk at room temperature for 1 hr and subsequently incubated for 1 hr with the antibodies against hTTL, Tyr-tubulin, Glu-tubulin, Δ2-tubulin, α-tubulin (5H1; PharMingen, San Diego, CA) and actin (20-33; Sigma Chemical, St. Louis, MO). The filter was further incubated with horseradish peroxidase-conjugated mouse or rabbit IgG secondary antibody (Cell Signaling Technologies, Beverly, MA). Immunoreactivity was detected using the enhanced chemiluminescence system (ECL; Amersham Pharmacia Biotechnology, Uppsala, Sweden) according to the manufacturer's instructions. The films were exposed at multiple time points to ensure that the images were not saturated.

Immunohistochemistry

Immunohistochemical stainings with antibodies against hTTL (1:100), Tyr-tubulin (1:100), Glu-tubulin (1:100) and Δ2-tubulin (1:100) were performed on 10 human neuroblastoma tumors selected from the surgical pathology file at the Department of Pathology, Aichi Medical University, based on the results of histopathology evaluation[26] and *MYCN* status. Also performed were immunostainings with antibodies against TrkA (1:40, 763; Santa Cruz Biotechnology, Santa Cruz, CA), CD56 (1B6; Novocastra Laboratories, Peterborough, U.K.) and Ki-67 (1:200, MIB-1; Dako, Kyoto, Japan) on the same tumor tissues. All of those tumor samples were obtained prior to chemotherapy and irradiation therapy and included 6 favorable histology cases with nonamplified *MYCN* (FH&NA) and 4 unfavorable histology cases with amplified *MYCN* (UH&A). Among the neuroblastoma cases, tumors in the FH&NA subset were reported to be the most favorable biologically and clinically. In contrast, tumors in the UH&A subset are known to be the most aggressive with the poorest clinical outcome.[27] Four μm thick sections from the formalin-fixed and paraffin-embedded tissue samples were deparaffinized and microwaved for 3 × 5 min in Na-citrate buffer (pH 6.0) for antigen retrieval. The slides were first immersed in 0.3% hydrogen peroxide in methanol for 20 min and then in 10% normal goat serum for 30 min. The primary antibodies were then applied at 4°C overnight, followed by a standard staining procedure using the Vectastain ABC kit (Vector Laboratories, Burlingame, CA). Sections were counterstained with hematoxylin for light microscopic review and evaluation. hTTL, Tyr-tubulin, Glu-tubulin and Δ2-tubulin were always positively detected in the cytoplasm and neuritic processes of normal ganglion cells in the separate positive control sections as well as in the test sections as built-in control, whenever available. As for the negative controls of hTTL, Tyr-tubulin, Glu-tubulin, Δ2-tubulin and TrkA stainings, normal rabbit immunoglobulins (1:500 dilution, Vector Laboratories) were applied as the primary antibody. As for the negative controls of CD56 and Ki-67 stainings, we followed the staining procedure without the primary antibodies.

Statistical analysis

Student's *t*-tests were used to explore possible associations between *hTTL* expression and other factors, such as age. Since the values of the *hTTL* expression were skewed, a log transformation was used to achieve the normality when using *t*-test and Cox regression. The distinction between high and low levels of *hTTL* was based on the median value (low, *hTTL* < 95 e.u.; high, *hTTL* > 95 e.u.), regardless of tumor stage, *MYCN* copy number, or survival. Kaplan-Meier survival curves were calculated, and survival distributions were compared using the log-rank test. Cox regression models were used to explore associations between *hTTL* expression, age, *MYCN* amplification, mass screening, origin and survival. Statistical significance was declared if the *p*-value was < 0.05. Statistical analysis was performed using Stata 7.0. (Stata, College Station, TX).

RESULTS

Cloning and expression of hTTL *gene*

We have previously constructed oligo-capping cDNA libraries from 3 fresh human NBL tissues (stages 1 and 2, high *TrkA* expression and a single copy of *MYCN*), which were gradually undergoing spontaneous regression probably due to neuronal apoptosis.[20] Screening of 1,152 novel genes by reverse transcriptase (RT)-PCR revealed that 194 genes were expressed differentially between NBLs with favorable prognosis and those with unfavorable outcome. Among them, we detected a partial cDNA sequence (*Nbla00660*) corresponding to the human ortholog of *tubulin tyrosine ligase* (*hTTL*) gene. We then cloned the full-length *hTTL* cDNA using both conventional phage library screening and genome sequence-based RT-PCR procedure. The *hTTL* gene was mapped to chromosome 2q13 and consisted of 7 exons (Fig. 2*a*) with 377 predicted amino acids (Genbank/DDBJ accession number AB071393; Fig. 2*b*). Comparison of the deduced amino acid sequence of human *TTL* cDNA with those of mouse, rat, pig and cow showed identity by 94%, 94%, 93% and 94%, respectively. *hTTL* was ubiquitously expressed in various human tissues including heart, kidney, lung, colon, thymus, spleen, mammary gland, testis, prostate, brain, cerebellum, liver, fetal brain, fetal liver, adrenal gland and skeletal muscle (Fig. 2*c*). However, it was rather preferentially expressed in adult and fetal brains and lung.

Specific antibodies and catalytic activity of hTTL

To study the role of hTTL and the tyrosination/detyrosination cycle regulated by TTL in neuroblastoma, we generated specific antibodies against human Tyr-tubulin, Glu-tubulin and Δ2-tubulin based on the previous reports.[16,18,28] The PVDF membranes spotted with equal amount (1 μg) of synthetic peptides corresponding to COOH terminal 7 amino acid residues of Tyr-tubulin (CEEEGEEY), Glu-tubulin (CGEEEGEE) and Δ2-tubulin (CEGEEEGE) were immunoblotted with rabbit anti-Tyr-tubulin antibody (Fig. 3*a*, top), anti-Glu-tubulin antibody (Fig. 3*a*, middle) and anti-Δ2-tubulin antibody (Fig. 3*a*, bottom), respectively. There were no crossreactivities among them, suggesting that those 3 antibodies were highly specific to each form of tubulin. To confirm the catalytic activity of hTTL encoded by the gene we cloned, we transfected the HEK293T cells with various amount of *hTTL* expression construct. Increased levels of hTTL in those cells induced tyrosination of tubulin in dose-dependent manner, while the level of endogenous Glu-tubulin was decreased (Fig. 3*c*). These results showed that hTTL protein encoded by the gene we cloned has its catalytic activity.

Upregulation of hTTL expression during neuronal differentiation

BMP2 has been characterized as a neurotrophic factor.[29] Recently, Nakamura *et al.*[30] have reported that RTBM1, a human neuroblastoma cell line, is responsive to both BMP2 and RA by extending neurites. By using this system, we examined whether the expression levels of hTTL change during induction of neuronal differentiation. As shown in Figure 4, the treatment of RTBM1

a

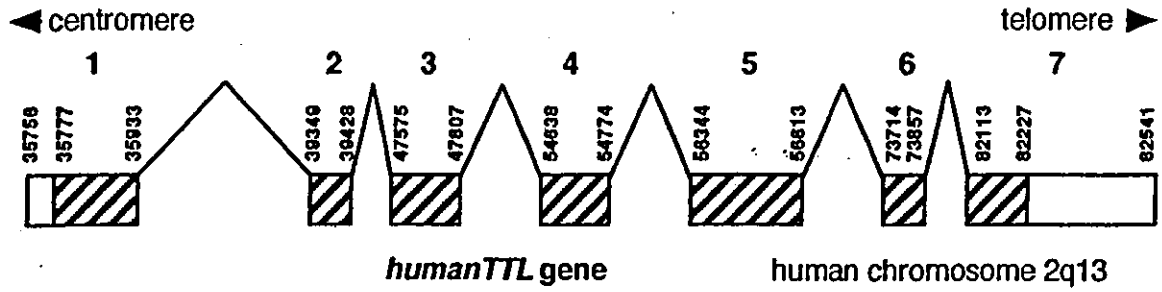

b

```
humanTTL  MYTFVVRDENSSVYAEVSRLLLATGHWKRLRRDNPRFNLMLGERNRLPFGRLGHEPGLVQLVNYYRGADKLCRKAS 76
mouseTTL  MYTFVVRDENSSVYAEVSRLLLATGYWKRLRRDNPRFNLMLGERNRLPFGRLGHEPGLAQLVNYYRGADKLCRKAS 76
ratTTL    MYTFVVRQENSSVYAEVSRLLLATGYWKRLRRDNPRFNLMLGGRNRLPFGRLGHEPGLAQLVNYYRGADKLCRKAS 76
pigTTL    MYTFVVRDENSSVYAEVSRLLLATGHWKRLRRDNPRFNLMLGERNRLPFGRLGHEPGLMQLVNYYRGADKLCRKAS 76
cowTTL    MYTFVVRDENSSVYAEVSRLLLATGHWKRLRRDNPRFNLMLGERNRLPFGRLGHEPGLMQLVNYYRGADKLCRKAS 76
          ******* ****************** ****************** ****************** ******************

humanTTL  LVKLIKTSPELAESCTWFPESYVIYPTNLKTPVAPAQNGIQPPISNSRTDEREFFLASYNRKKEDGEGNVWIAKSS 152
mouseTTL  LVKLVKTSPELSESCSWFPESYVIYPTNLKTPVAPAQNGIQLPVSNSRTDEREFFLASYNRKKEDGEGNVWIAKSS 152
ratTTL    LVKLVKTSPELSESCSWFPESYVIHPTNLKTPVAPAQNGIQLPVSNSRTDEREFFLASYNRKKEDGEGNVWIAKSS 152
pigTTL    LVKLIKTSPELAESCTWFPESYVIYPTNLKTPVAPAQNGIHPPIHSSRTDEREFFLTSYNKKKEDGEGNVWIAKSS 152
cowTTL    LVKLIKTSPELAESCTWFPESYVIYPTNLKTPVAPAQDGIHPPLHSSRTDEREFFLASYNRKKEEGEGNVWIAKSS 152
          **** ****** *** ******** ************ ** *  ********** *** *** ************

humanTTL  AGAKGEGILISSEASELLDFIDNQGQVHVIQKYLEHPLLLEPGHRKFDIRSWVLVDHQYNIYLYREGVLRTASEPY 228
mouseTTL  AGAKGEGILISSEASELLDFIDSQGQVHVIQKYLERPLLLEPGHRKFDIRSWVLVDHQYNIYLYREGVLRTASEPY 228
ratTTL    AGAKGEGILISSEASELLDFIDNQGQVHVIQKYLEHPLLLEPGHRKFDIRSWVLVDHQYNIYLYREGVLRTASEPY 228
pigTTL    AGAKGEGILISSEATELLDFIDNQGQVHVIQKYLERPLLLEPGHRKFDIRSWVLVDHQYNIYLYREGVLRTASEPY 228
cowTTL    AGAKGEGILISSDATELLDFIDNQGQVHVIQKYLERPLLLEPGHRKFDIRSWVLVDHQFNIYLYREGVLRTASEPY 228
          ************ * ******* ************ ********************** ******************

humanTTL  HVDNFQDKTCHLTNHCIQKEYSKNYGKYEEGNEMFFKEFNQYLTSALNITLESSILLQIKHIIRNCLLSVEPAIST 304
mouseTTL  HVDNFQDKTCHLTNHCIQKEYSKNYGKYEEGNEMFFEEFNQYLTSALNITLESSILLQIKHIIRSCLMSVEPAIST 304
ratTTL    HVDNFQDKTCHLTNHCIQKEYSKNYGKYEEGNEMFFEEFNQYLTSALNITLENSILLQIKHIIRSCLMSVEPAIST 304
pigTTL    HTDNFQDKTCHLTNHCIQKEYSKNYGKYEEGNEMFFEEFNQYLTSALNITLESSILLQIKHIIRSCLLSVEPAIST 304
cowTTL    HMDNFQDKTCHLTNHCIQKEYSKNYGKYEEGNEMFFEAFNRYLTSALNITLESSILLQIKHIIRSCLMSVEPAIST 304
          * ************************************  ** ************ ************ ** ********

humanTTL  KHLPYQSFQLFGFDFMVDEELKVWLIEVNGAPACAQKLYAELCQGIVDIAISSVFPPPDVEQPQTQP--AAFIKL  377
mouseTTL  KHLPYQSFQLLGFDFMVDEELKVWLIEVNGAPACAQKLYAELCQGIVDIAISSVFPPPDTEQVPQQP--AAFVKL  377
ratTTL    KHLPYQSFQLLGFDFMVDEELKVWLIEVNGAPACAQKLYAELCQGIVDIAISSVFPPPDTEQVPQQP--AAFMKL  377
pigTTL    RHLPYQSFQLFGFDFMVDEDLKVWLIEVNGAPACAQKLYAELCQGIVDIAIASVFPPPDAEQQQQQPPPAAFIKL  379
cowTTL    KHLPYQSFQLFGFDFMVDEELKVWLIEVNGAPACAQKLYAELCQGIVDIAIASVFPPPDAEQQPPQP--ATFIKL  377
          ********* ******** ********************************** ******* **   **  * * **
```

c

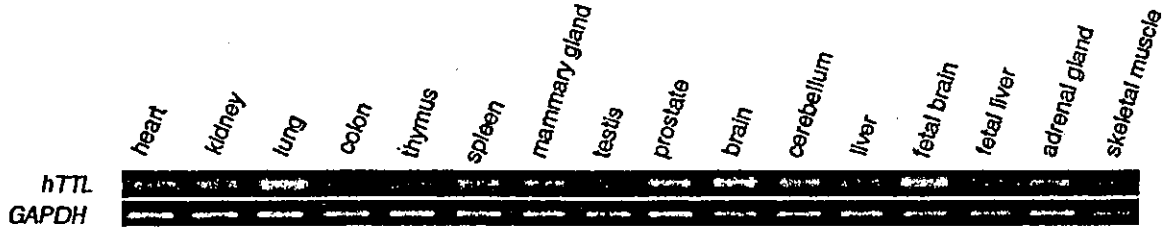

FIGURE 2

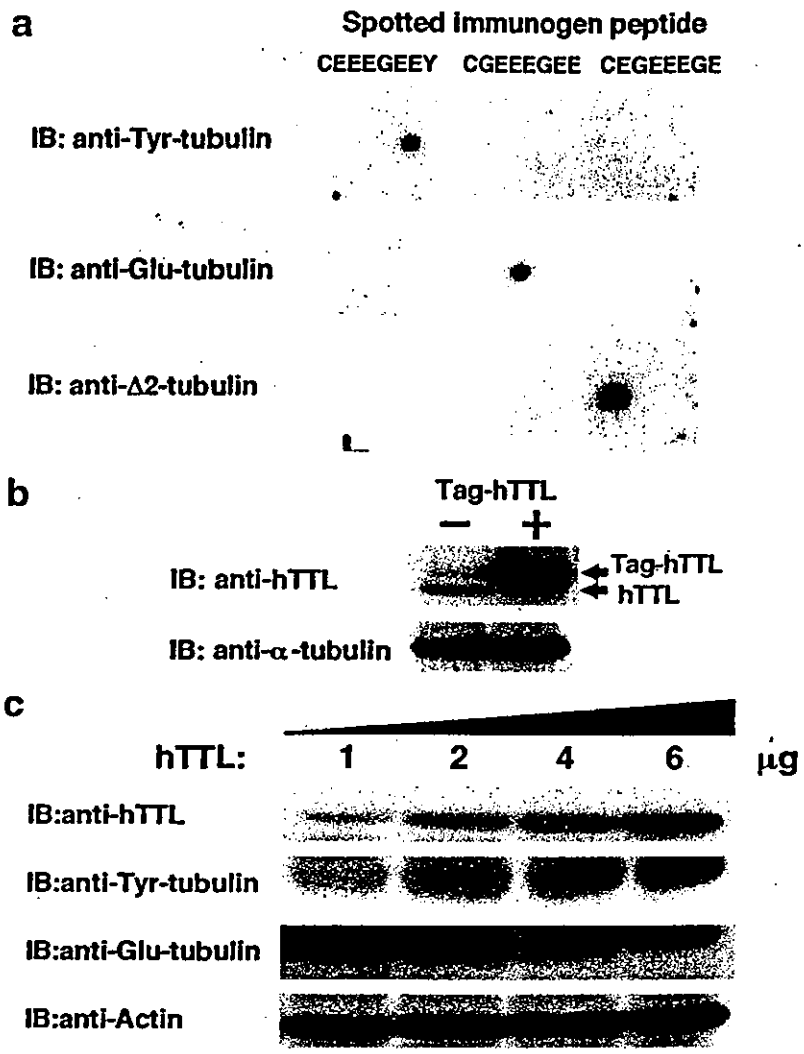

FIGURE 3 – hTTL has a tyrosination activity in mammalian cultured cells. (*a*) Specificity of antibodies. The indicated synthetic peptides were spotted on the filter and immunoblotted with the polyclonal anti-Tyr-tubulin (top), anti-Glu-tubulin (middle), or anti-Δ2-tubulin antibody (bottom). (*b*) Expression of FLAG-tagged hTTL. Whole-cell lysates prepared from COS7 cells transfected with the empty plasmid or with the expression plasmid for FLAG-tagged hTTL were subjected to immunoblotting with the anti-hTTL antibody (top). The expression level of α-tubulin was examined to ensure equal loading (bottom). (*c*) The exogenously expressed hTTL has a catalytic activity. HEK293T cells were transfected with increasing amounts of the hTTL expression plasmid. Forty-eight hours after transfection, whole-cell lysates were prepared and immunoblotted with the indicated antibodies. The expression level of actin is included as a loading control (bottom).

cells with 1 nM BMP2 or 5 μM RA induced remarkable morphologic differentiation by day 8. The hTTL protein level was increased after day 2 and peaked on day 6 in the former and on day 3 in the latter. Thereafter, it appeared to be decreased. Thus, hTTL was induced during induction of neuronal differentiation in NBL cells.

Expression of hTTL mRNA in primary neuroblastomas

To evaluate the clinical significance of *hTTL*, we examined the expression of *hTTL* mRNA in 16 favorable (stage 1, high expression of *TrkA* and a single copy of *MYCN*) and 16 unfavorable (stage 3 or 4, low expression of *TrkA* and amplification of *MYCN*) NBLs using semiquantitative RT-PCR. As shown in Figure 5(*a*), *hTTL* was preferentially expressed in favorable NBLs. Therefore, we next performed quantitative real-time RT-PCR to measure the levels of *hTTL* transcript in 74 primary NBLs. Table I shows the quantitative levels of *hTTL* mRNA expression (mean ± SEM) by age (< 1-year-old *vs.* ≥ 1-year-old), tumor stages (1 + 2 + 4s *vs.* 3 + 4), *TrkA* expression (low *vs.* high), *MYCN* gene copies (single *vs.* amplified), origin (adrenal gland *vs.* others), mass screening (tumors found by mass screening *vs.* sporadic tumors) and prognosis (alive *vs.* dead). High levels of *hTTL* expression were significantly associated with favorable stages ($p = 0.0069$), high *TrkA* expression ($p = 0.002$), a single copy of *MYCN* ($p < 0.00005$), tumors found by mass screening ($p = 0.0042$), origins other than adrenal gland ($p = 0.0042$) and a good prognosis ($p = 0.023$). *hTTL* expression was marginally associated with age. The log-rank test indicated that *hTTL* expression was associated with better survival ($p = 0.026$), which was also indicated in the Kaplan-Meier cumulative survival curves (Fig. 5*b*).

The univariate Cox regression was employed to examine the individual relationship of each variable to survival (Table II). Expression of *hTTL*, age, *MYCN* copy numbers and mass screening were found to be of prognostic importance, supporting the results of the log-rank test. However, since *hTTL* expression was highly associated with *MYCN*, mass screening and origin, multivariable Cox models were not fitted to assess the predictive importance of *hTTL* expression for survival after controlling these prognostic factors, suggesting that expression of *hTTL* was not an independent prognostic indicator.

FIGURE 2 – Genomic structure, alignment of amino acid sequence and mRNA expression of human *TTL*. (*a*) Genomic structure of *hTTL*. The *hTTL* gene that is mapped to 2q13 consists of 7 exons. Untranslated regions (open boxes) and coding regions (hatched boxes) are shown. Numbers indicate nucleotide position in human BAC clone *RP11-1I24* (accession number AC012442). (*b*) Comparison of amino acid sequences among mammalian TTLs. The gaps produced by the alignment are indicated by a hyphen in the sequence. The conserved amino acid residues in TTLs are shown by asterisks below the alignment. (*c*) Tissue distribution of *hTTL* mRNA. The expression levels of *hTTL* mRNA in the indicated human tissues were examined by semiquantitative RT-PCR (top). *GAPDH* expression was also examined as an internal control (bottom).

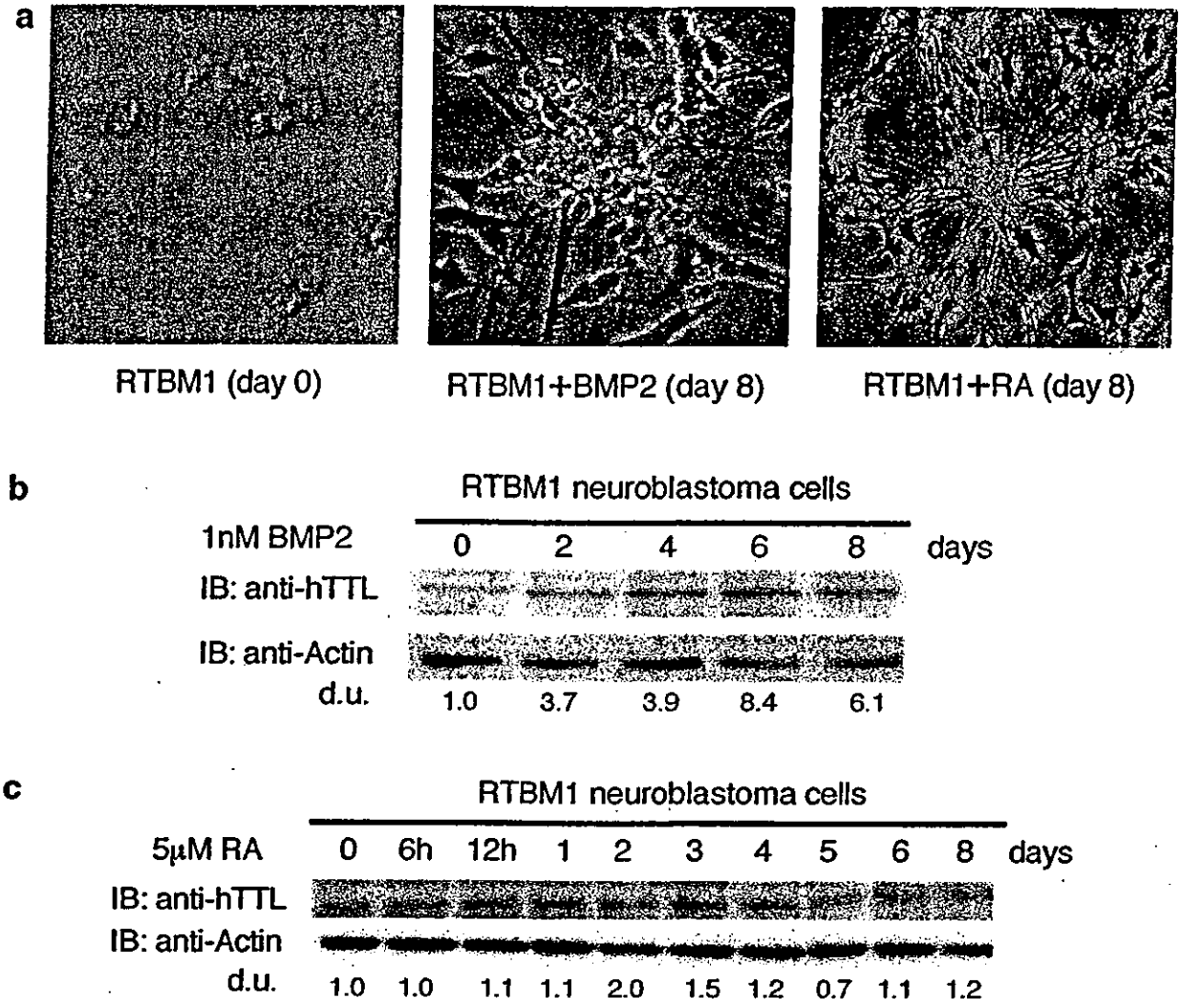

FIGURE 4 – TTL is induced during BMP2- and RA-mediated neuroblastoma differentiation. (*a*) BMP2- or RA-induced morphologic changes in RTBM1 neuroblastoma cells. RTBM1 cells were treated with BMP2 or RA at a final concentration of 1 nM or 5 μM, respectively, and maintained for 8 days. (*b*) Expression levels of hTTL are increased in response to BMP2. At the indicated time points after the treatment with BMP2 (at a final concentration of 1 nM), whole-cell lysates prepared from RTBM1 cells were subjected to immunoblotting with the antibody against hTTL (top). Actin protein levels were determined as a loading control (bottom). (*c*) Induction of hTTL in response to RA. RTBM1 cells were exposed to RA at a final concentration of 5 μM. Whole-cell lysates were prepared at the indicated time points after the treatment with RA and subjected to immunoblotting with the anti-hTTL (top) or with antiactin (bottom) antibody. d.u., arbitrary density units.

Immunohistochemistry

To determine the expression pattern of hTTL protein in primary NBLs, we performed immunohistochemical study for 6 favorable (stage 1 or 2 and a single copy of *MYCN*) and 4 unfavorable (stage 3 or 4 and amplified *MYCN*) NBLs. hTTL, Tyr-tubulin and Glu-tubulin were positively detected both in the cytoplasm of the neuroblastic cells and in the fine meshwork of neuropil of all 6 tumors with favorable histology (Shimada's classification) and a single copy of *MYCN* (Fig. 6*a–c*). In contrast, all 4 tumors with unfavorable histology and *MYCN* amplification were negative for Tyr-tubulin and Glu-tubulin, and only 1 tumor in this subset was positive for hTTL (Fig. 6*f–h*). Interestingly, all 10 NBL tumors were positive for Δ2-tubulin, but whose staining pattern was rather distinct in different subsets of the tumors. In the favorable tumors, Δ2-tubulin showed a localization similar to hTTL, Tyr-tubulin and Glu-tubulin and was detected in the cytoplasm and in the fine neuropil (Fig. 6*d*). On the other hand, Δ2-tubulin in the aggressive tumors was found only in the cytoplasm of neuroblastic cells, since they had no or a very limited capability of neuritic process production (*i.e.*, neuropil formation; Fig. 6*i*).

CD56 was detected in all 10 tumors, regardless of the histology and *MYCN* status (data not shown). TrkA was detected in all of 6 favorable tumors (Fig. 6*e*), but was negative in 3 of 4 aggressive tumors (Fig. 6*j*). It was noted that one unfavorable tumor with weakly positive trkA showed positive staining for TTL. Ki-67 staining revealed 10–20% and 60–70% positive cells in the favorable and the unfavorable tumors, respectively (data not shown).

DISCUSSION

In the present study, we have identified human ortholog of *tubulin tyrosine ligase* gene, which is highly conserved among the mammalian species. *hTTL* mRNA is ubiquitously expressed but rather preferential in both fetal and adult brains as well as in lung. The specific antibodies raised against hTTL, Tyr-tubulin, Glu-tubulin and Δ2-tubulin have confirmed the catalytic activity of